Surface and Interface X-ray Scattering

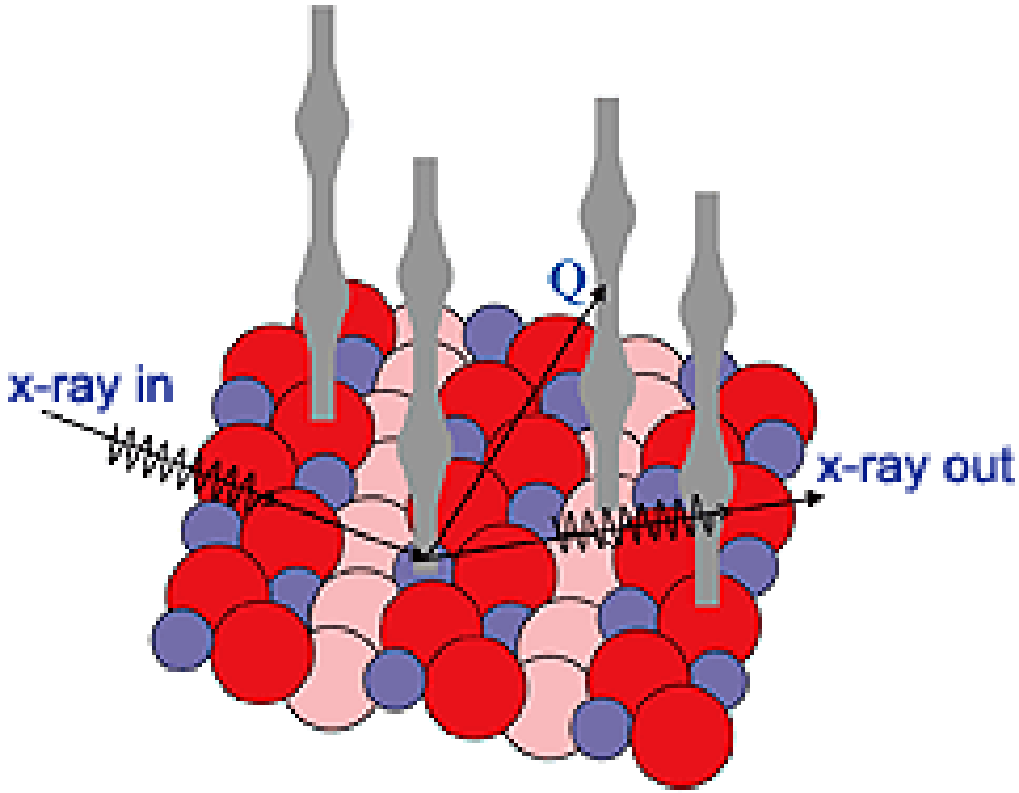

Tom Trainor (fftpt@uaf.edu)

University of Alaska Fairbanks

1st Annual SSRL Workshop on Synchrotron X-ray Scattering Techniques in Materials and Environmental Sciences

Surface and Interface Scattering: Why bother?

- Interface electron density profiles (Å-scale resolution)
- Surface and interface roughness / correlation lengths
- **Interface structure/surface crystallography (1-D & 3-D)**
    - Dependence on chemical/physical conditions
    - Growth/dissolution mechanisms and kinetics
    - Structure/binding modes of adsorbates
    - Structure reactivity relationships
    - and ……

Why x-rays?

- Large penetration depth → experiments can be done in-situ
    - Liquid water, controlled atmospheres, growth chamber, etc…
- Kinematic scattering → relatively straightforward analysis
- Downside?
    - Weak signals in general → need synchrotron x-rays

Outline

- A brief example
- Crystal Truncation Rod – what the heck is that ??
- Influence of surface structure
- Measurements
- More examples

Example: Hematite (0001) Surface Terminations and rxn with H_2O

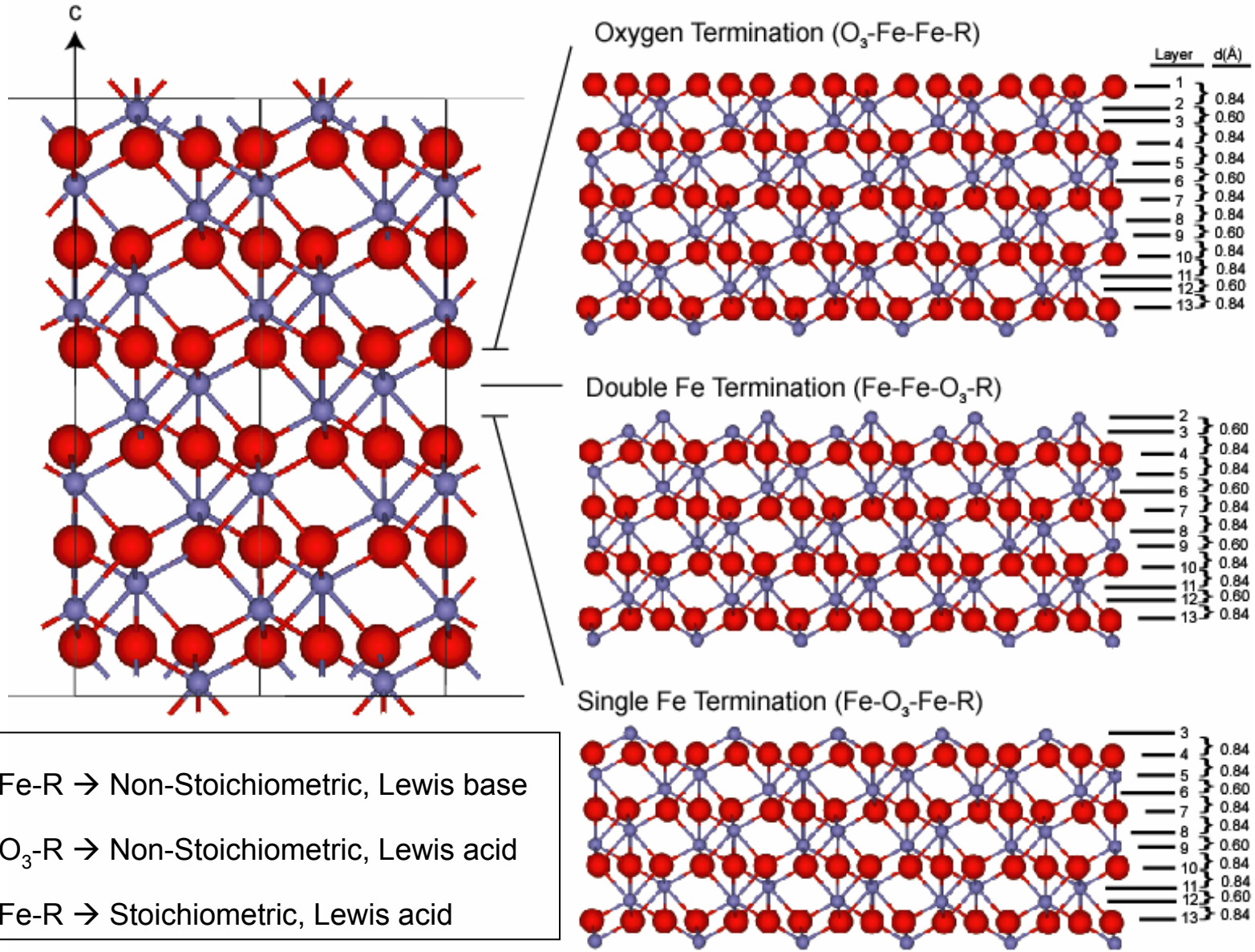

O_3-Fe-Fe-R → Non-Stoichiometric, Lewis base

Fe-Fe-O_3-R → Non-Stoichiometric, Lewis acid

Fe-O_3-Fe-R → Stoichiometric, Lewis acid

Example: Hematite (0001) Surface Terminations and Rxn with H_2O

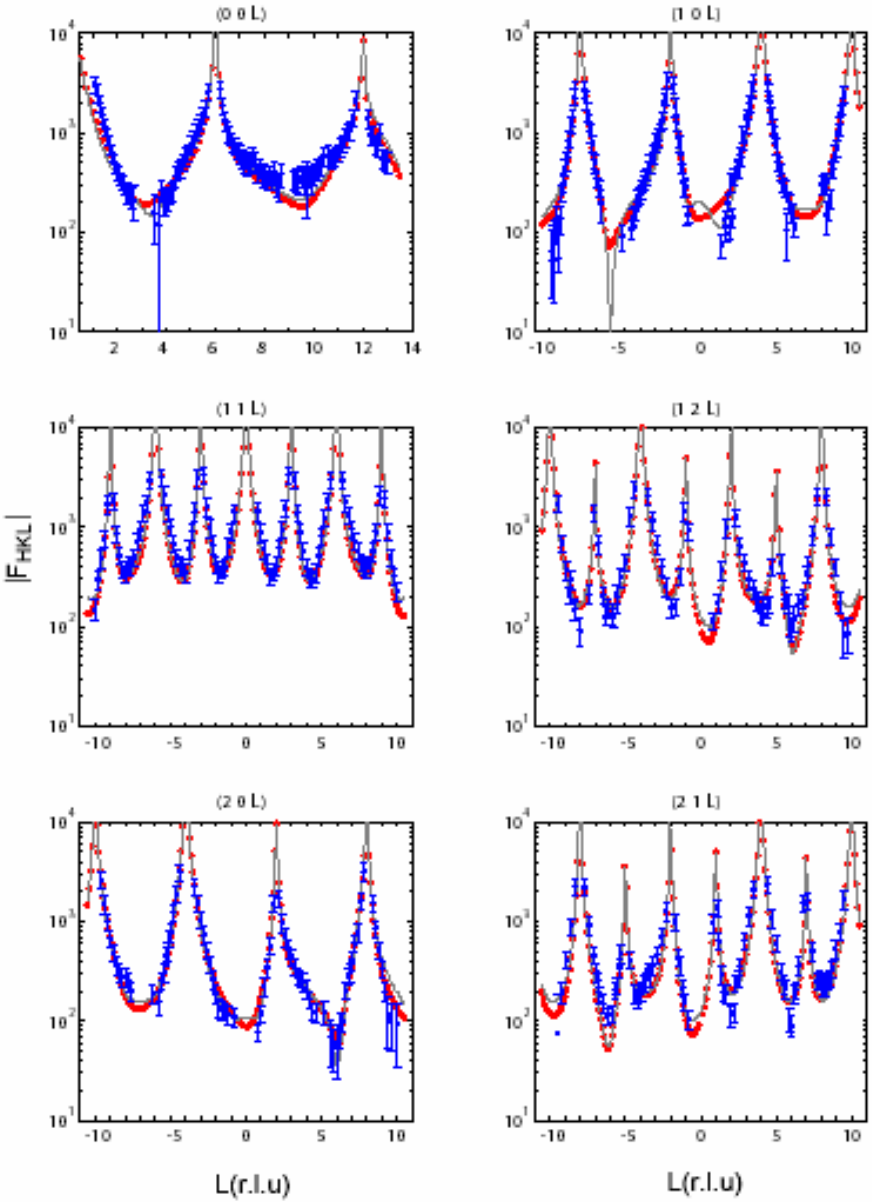

Surface scattering (CTR) data and best fit model(s)

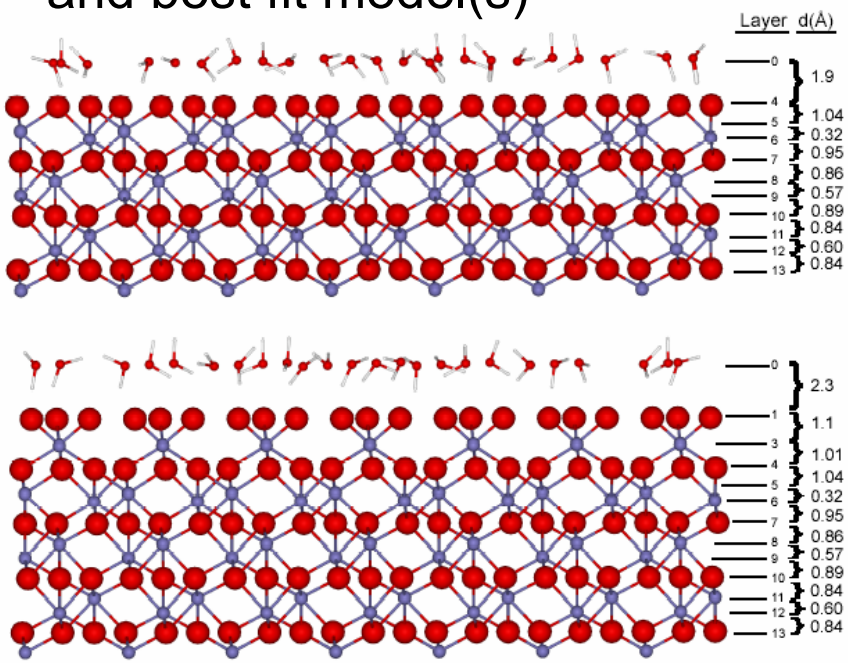

So what?

- Structural characterization of the predominant chemical moieties present at the <u>solid-solution</u> interface

→ controls on interface reactivity.

What's a crystal truncation rod? The short version…

Scattering intensity that arises between bulk Bragg peaks due to the presence of a sharp termination of the crystal lattice (i.e. a surface). The direction of the scattering intensity is perpendicular to the surface and is a sensitive function of surface/interface structure.

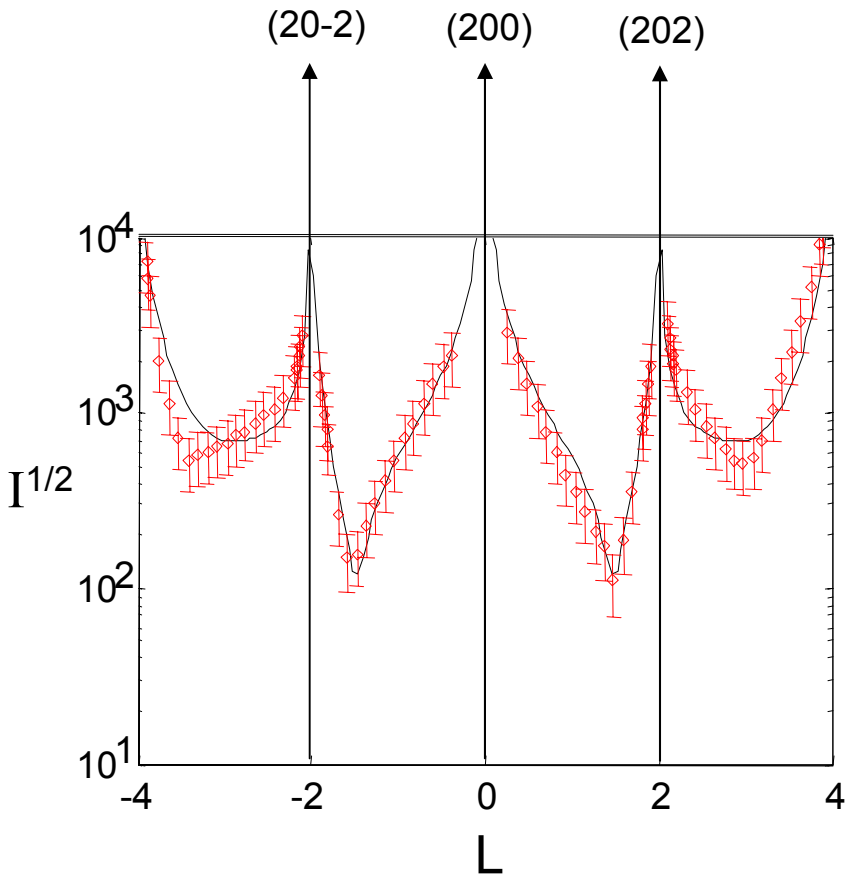

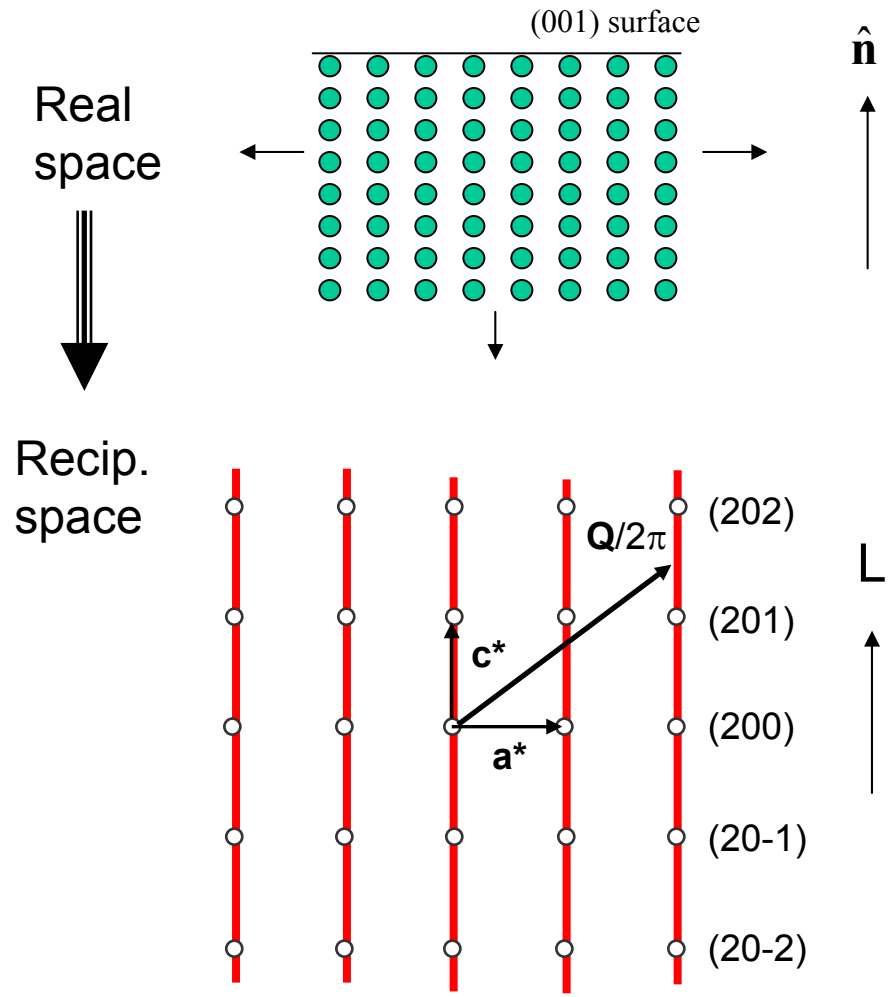

What's a crystal truncation rod? The quantitative (long!) explanation…

Lets go back to some x-ray scattering basics and recall: *the scattered intensity is proportional to the square modulus of the Fourier transform of the electron density*

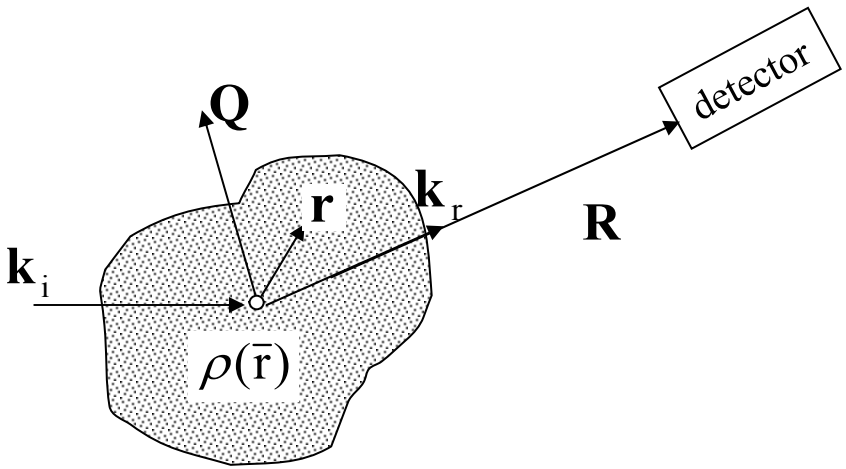

$$I_{det} = \mathbf{E}\ \ \mathbf{E}^* \propto \frac{E_o^2\, r_e^2}{R^2} \left| FT\left[\rho(\mathbf{r})\right] \right|^2$$

$$FT\left[\rho(\mathbf{r})\right] \propto \int \rho(\mathbf{r})\, e^{i\,\mathbf{Q}\bullet\mathbf{r}}\, dV$$

$$\downarrow$$

$$FT\left[\rho(\mathbf{r})\right] \propto \sum_n f_{a,n}\, e^{i\,\mathbf{Q}\bullet\mathbf{r}_n}$$

$$f_{a,n} = \int \rho_n(\mathbf{r})\, e^{i\,\mathbf{Q}\bullet\mathbf{r}}\, dV$$

$$I = \left|E(R)\right|^2 \propto \left| \sum_n f_{a,n}\, e^{i\,\mathbf{Q}\bullet\mathbf{r}_n} \right|^2$$

Sum is over all atoms at $\mathbf{r_n}$
$f_{a,n}$ are atomic scattering factors

Take advantage of periodicity of a crystal to simplify $\mathbf{r_n}$

Atoms in a unit cell

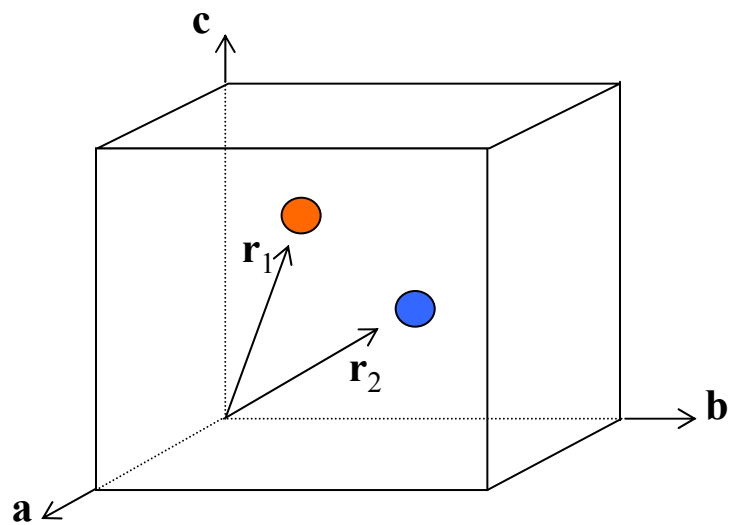

Unit cells in a crystal

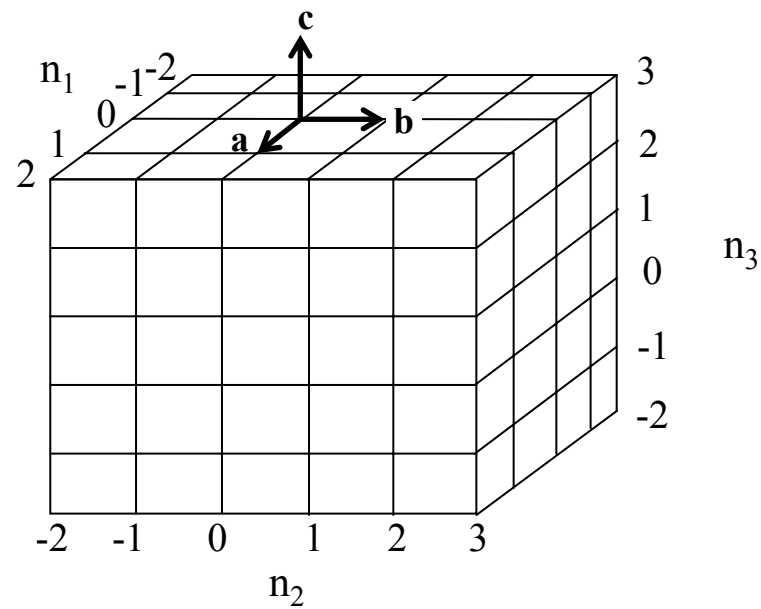

Position of the j'th atom in the cell is given by its <u>fractional coordinates:</u>

$$\mathbf{r}_j = x\,\mathbf{a} + y\,\mathbf{b} + z\,\mathbf{c}$$

Position of the $(n_1 n_2 n_3)$ unit cell is given by:

$$\mathbf{R}_c(n_1 n_2 n_3) = n_1\,\mathbf{a} + n_2\,\mathbf{b} + n_3\,\mathbf{c}$$

The position of the n'th atom in the xtal is:

$$\mathbf{r}_n = \mathbf{R}_c(n_1 n_2 n_3) + \mathbf{r}_j(xyz)$$

Real Space Planes ←→ Reciprocal Space Points

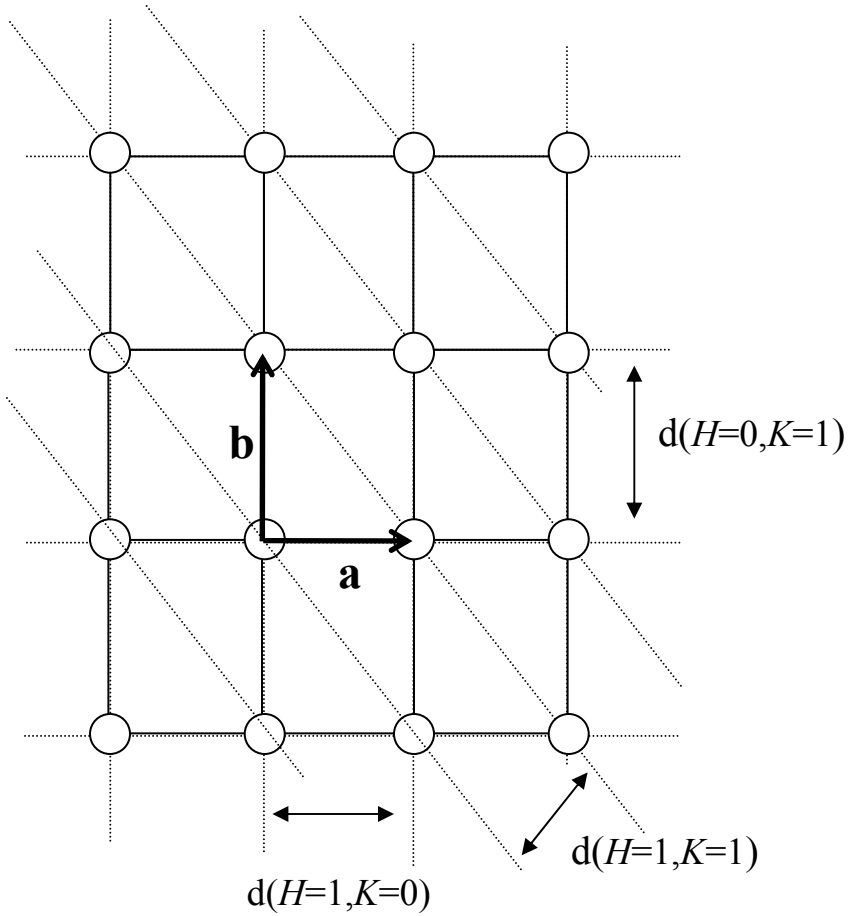

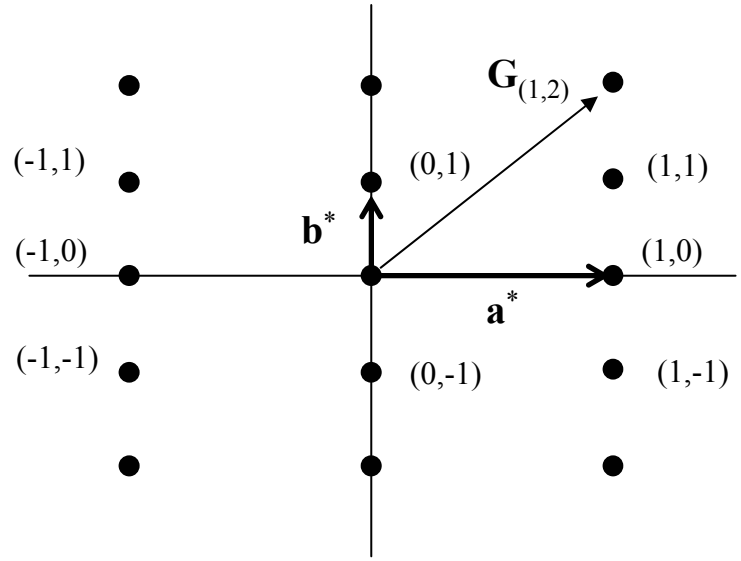

$$\mathbf{G} = H\,\mathbf{a}^* + K\,\mathbf{b}^* + L\,\mathbf{c}^*$$

$$|\mathbf{G}_{HKL}| = 1/\mathrm{d}_{HKL}, \quad \perp (HKL)$$

$$\mathbf{a}^* = \frac{\mathbf{b}\times\mathbf{c}}{\mathbf{a}\bullet\mathbf{b}\times\mathbf{c}} \qquad \mathbf{a}\bullet\mathbf{a}^* = 1$$

$$\mathbf{b}^* = \frac{\mathbf{c}\times\mathbf{a}}{\mathbf{a}\bullet\mathbf{b}\times\mathbf{c}} \qquad \mathbf{a}\bullet\mathbf{b}^* = \mathbf{a}\bullet\mathbf{c}^* = 0$$

$$\mathbf{c}^* = \frac{\mathbf{a}\times\mathbf{b}}{\mathbf{a}\bullet\mathbf{b}\times\mathbf{c}} \qquad \text{etc...}$$

(HKL) defines a plane with intercepts: $\dfrac{\mathbf{a}}{H}, \dfrac{\mathbf{b}}{K}, \dfrac{\mathbf{c}}{L}$

Express **Q** in terms of reciprocal lattice coordinates

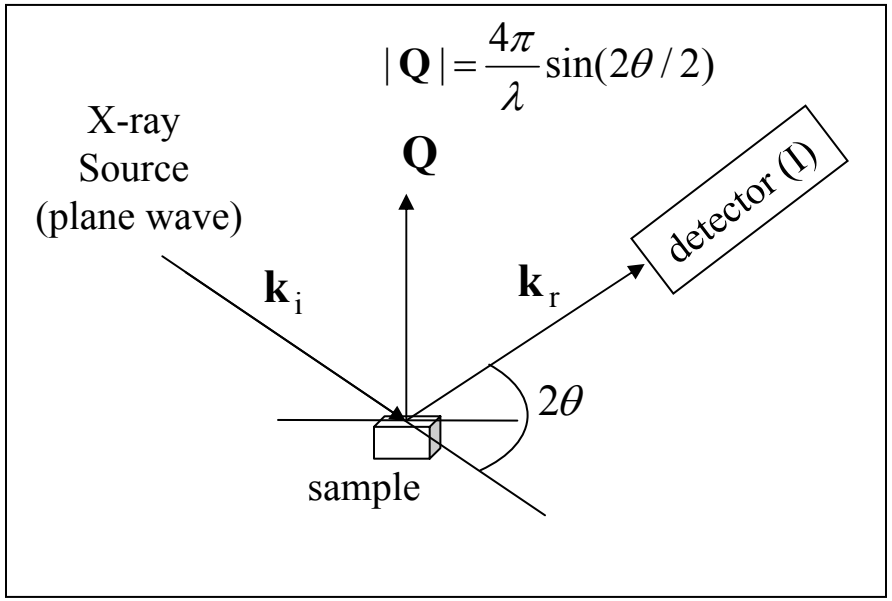

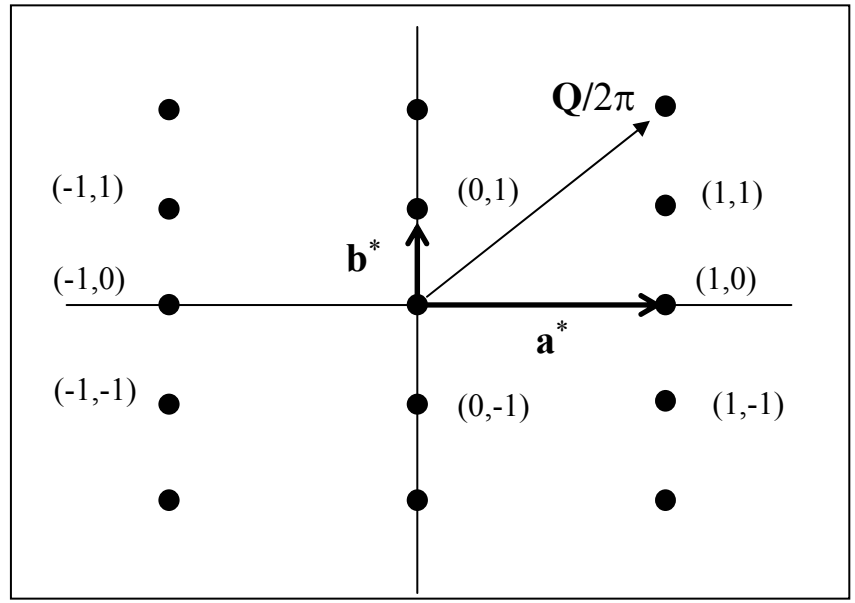

- **Q** as a vector in reciprocal space

$$\mathbf{Q} = 2\pi\,\mathbf{G} = 2\pi\left(H\,\mathbf{a}^* + K\,\mathbf{b}^* + L\,\mathbf{c}^*\right)$$

$$|\mathbf{Q}| = 2\pi\,|\mathbf{G}| = \frac{2\pi}{\mathrm{d}_{HKL}}$$

- Dot products in sum become simple to evaluate

$$\mathbf{Q}\bullet\mathbf{r}_\mathrm{n} = \mathbf{Q}\bullet\mathbf{R}_\mathrm{c} + \mathbf{Q}\bullet\mathbf{r}_\mathrm{j}$$

$$\mathbf{Q}\bullet\mathbf{r}_\mathrm{j} = 2\pi(\mathrm{x}\,H + \mathrm{y}\,K + \mathrm{z}\,L)$$

$$\mathbf{Q}\bullet\mathbf{R}_\mathrm{c} = 2\pi(\mathrm{n}_1\,H + \mathrm{n}_2\,K + \mathrm{n}_3\,L)$$

Substitute for $\mathbf{r}_n$ and $\mathbf{Q}$ in the summation over all atoms:

$$E(\mathbf{R}) \propto \quad FT[\rho(\mathbf{r})] = \sum_n f_{a,n} e^{i\,\mathbf{Q}\bullet\mathbf{r}_n}$$

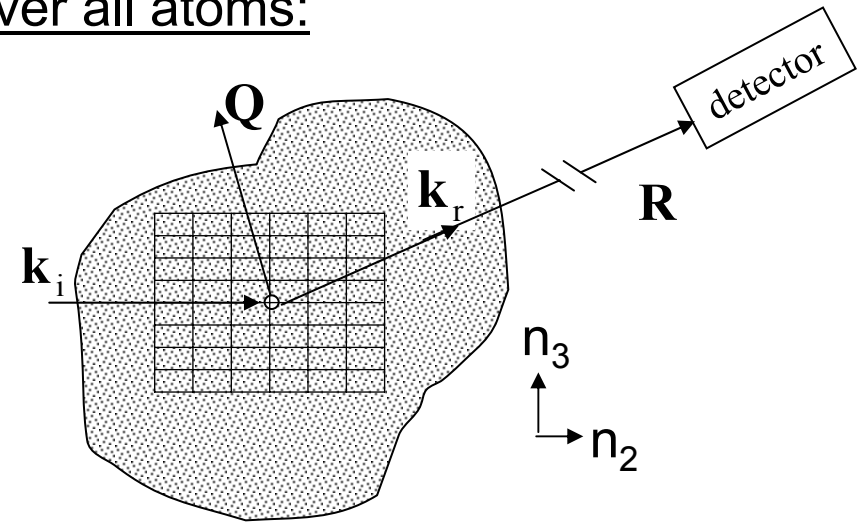

Sum over n_1, N_1 total cells

Sum over n_2, N_2 total cells

Sum over n_3, N_3 total cells

$$E \propto \sum_{-(N_1-1)/2}^{(N_1-1)/2} e^{i\,2\pi\, n_1 H} \sum_{-(N_2-1)/2}^{(N_2-1)/2} e^{i\,2\pi\, n_2 K} \sum_{-(N_3-1)/2}^{(N_3-1)/2} e^{i\,2\pi\, n_3 L} \sum_{j=1}^{m} f_{a,j} e^{i\,\mathbf{Q}\bullet\mathbf{r}_j} e^{-M_j}$$

Thermal disorder parameter

Sum over the m atoms in the unit cell

We can simplify to:

$$E \propto F_c S_1(H) S_2(K) S_3(L)$$

Structure factor of the unit cell

$$F_c = \sum_{j=1}^{m} f_{a,j} e^{i\,\mathbf{Q}\bullet\mathbf{r}_j} e^{-M_j}$$

Slit Function

$$S_1 = \sum_{-(N_1-1)/2}^{(N_1-1)/2} e^{i\,2\pi\, n_1 H} = \frac{\sin(N_1 \pi H)}{\sin(\pi H)}$$

$$\rightarrow N_1 \text{ as } H \rightarrow \text{integer}$$

Scattering intensity at a Bragg point

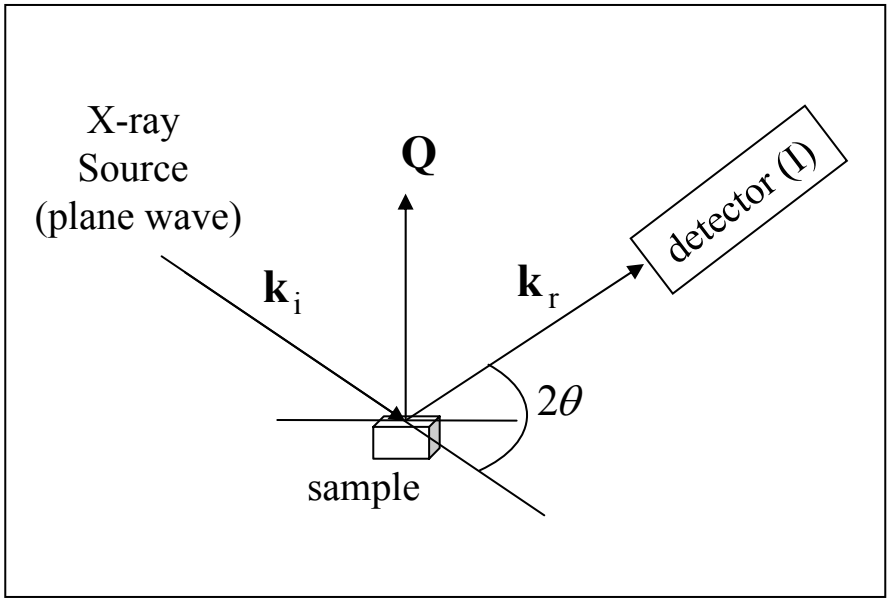

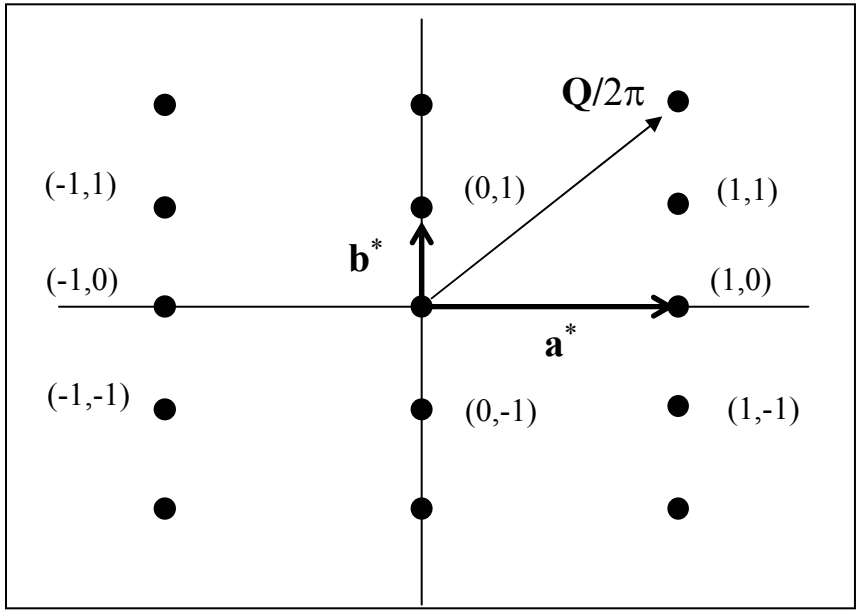

$$\mathrm{I} \propto |\mathrm{E}|^2 \propto |\mathrm{F}_c|^2 \frac{\sin^2(\mathrm{N}_1 \pi H)}{\sin^2(\pi H)} \frac{\sin^2(\mathrm{N}_2 \pi K)}{\sin^2(\pi K)} \frac{\sin^2(\mathrm{N}_3 \pi L)}{\sin^2(\pi L)} \rightarrow |\mathrm{F}_c|^2 N_1^2 N_2^2 N_3^2$$

For (HKL) → integer

What about the scattering away from Bragg peak (slit functions)

$$S_3(L) = \sum_{-(N_3-1)/2}^{(N_3-1)/2} e^{i\,2\pi\, n_3 L} = \frac{\sin(N_3 \pi L)}{\sin(\pi L)} \rightarrow N_3 \text{ as } L \rightarrow \text{integer}$$

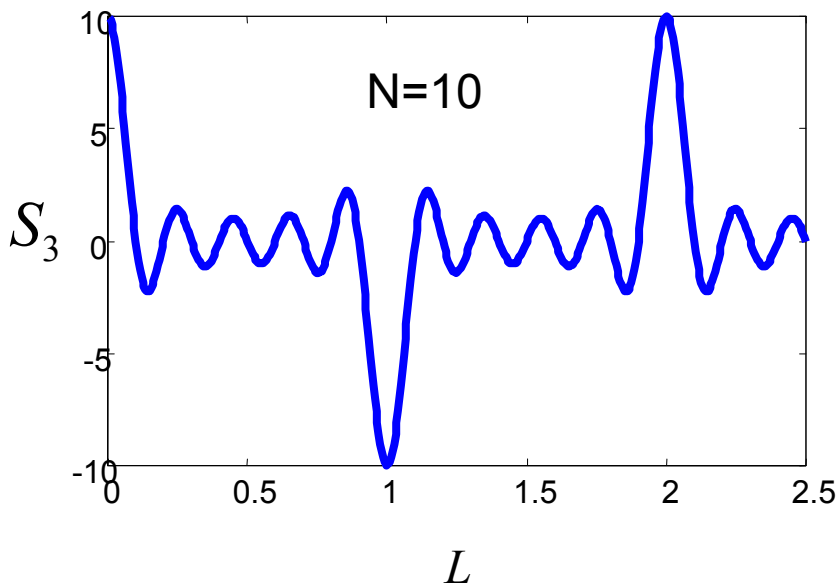

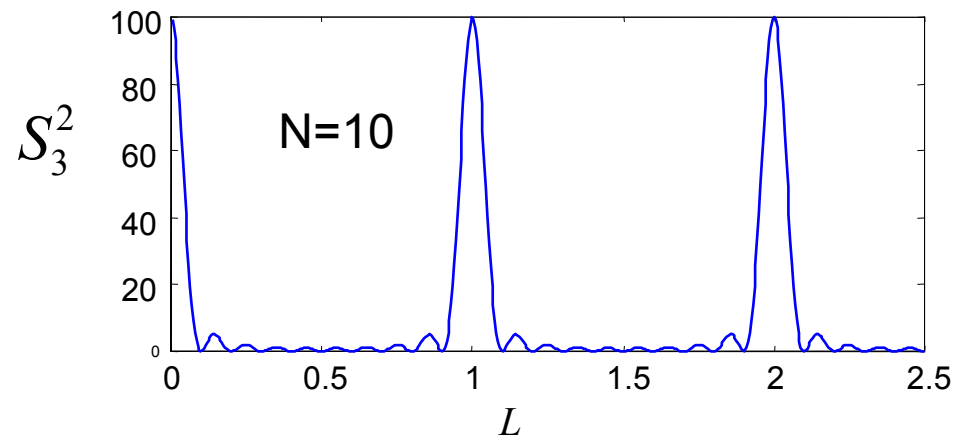

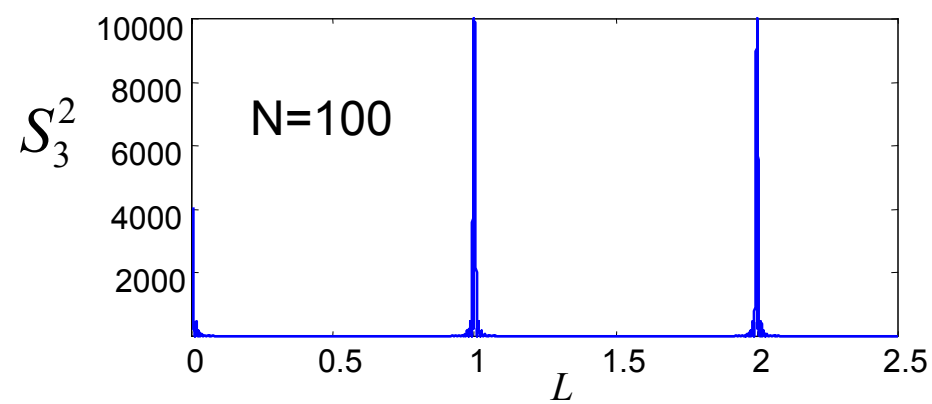

Intensity is nominal for non-integer values. But its not zero if the xtal is finite size!

Intensity variation between Bragg peaks is more evident on log scale.

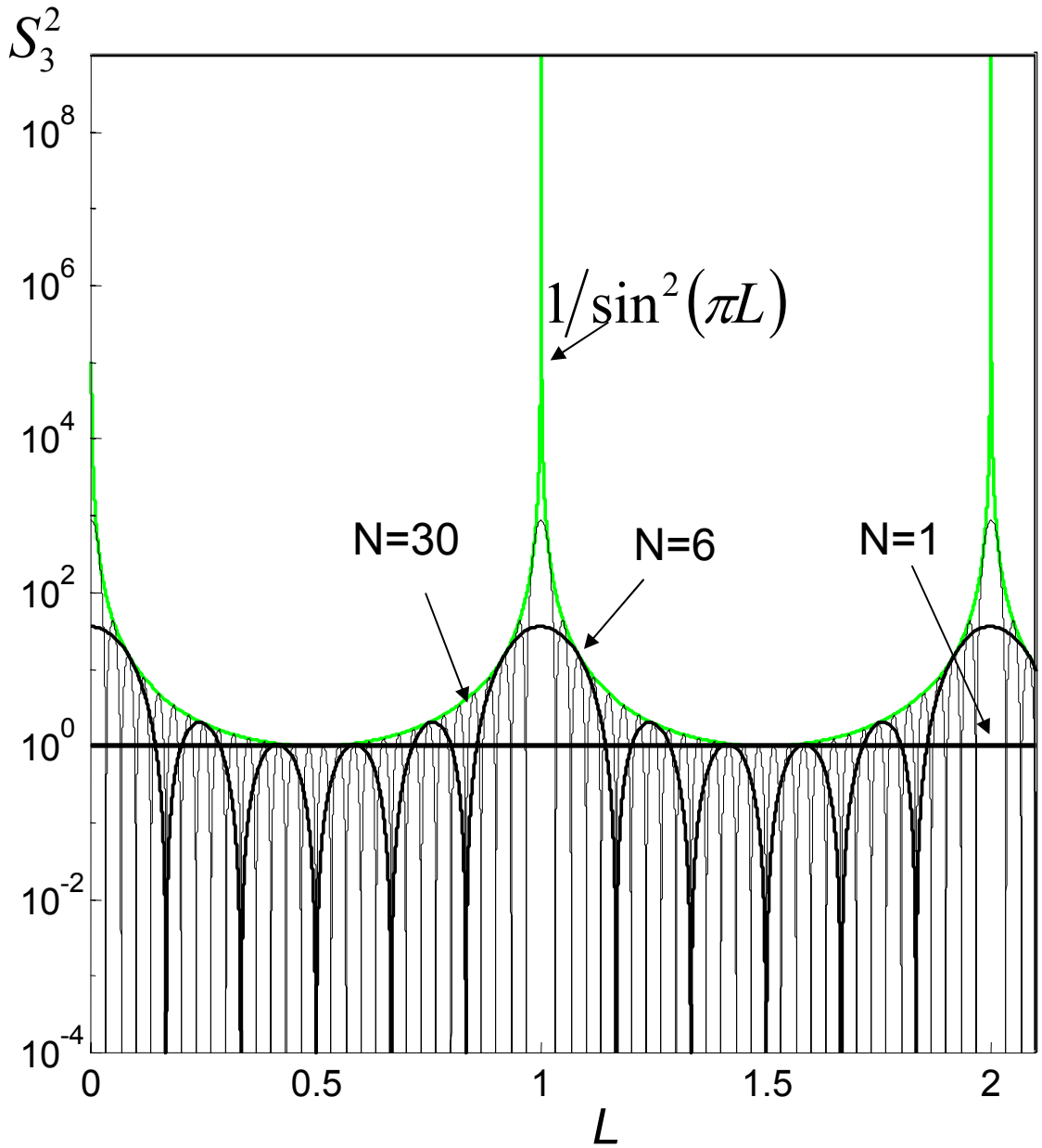

For N=1 no oscillations, scattering from a single layer.

Oscillations for N>1 due to interference between x-rays scattering from the top and bottom

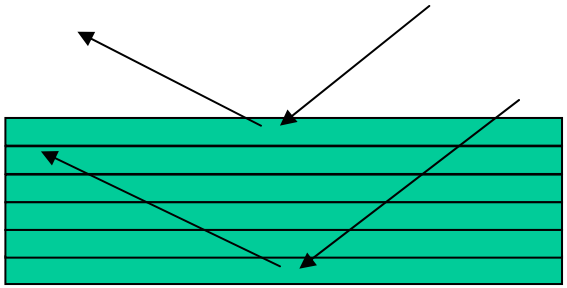

Intensity variation follows the $1/\sin^2$ profile

At mid-point (anti-Bragg) the intensity is the same as from a single layer!

The sharp boundaries of a finite size (i.e. small) crystal results in intensity between Bragg peaks

However, for a large single crystal in the Bragg geometry a better model for a surface is a semi-infinite stacking of slabs

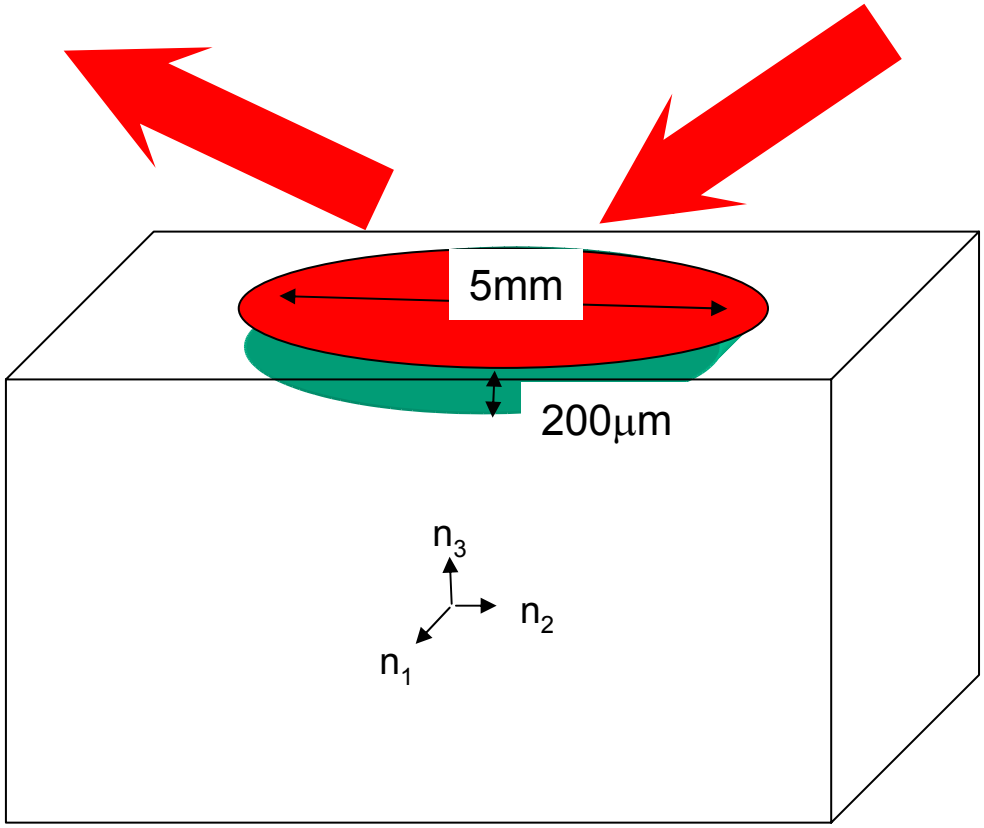

The crystal in this geometry appears infinite in-plane, and semi-infinite along the n_3 direction

Return to the sums and take large N_1 and N_2 and sum n_3 from 0 (the surface) to $-\infty$

$$E \propto F_c \sum_{-(N_1-1)/2}^{(N_1-1)/2} e^{i\,2\pi\, n_1 H} \sum_{-(N_2-1)/2}^{(N_2-1)/2} e^{i\,2\pi\, n_2 K} \sum_{-\infty}^{0} e^{i\,2\pi\, n_3 L}$$

$$\mathrm{Fctr} = \sum_{-\infty}^{0} e^{i\,2\pi\, n_3 L} = \frac{1}{(1-e^{-i\,2\pi\, L})}$$

(001) surface termination

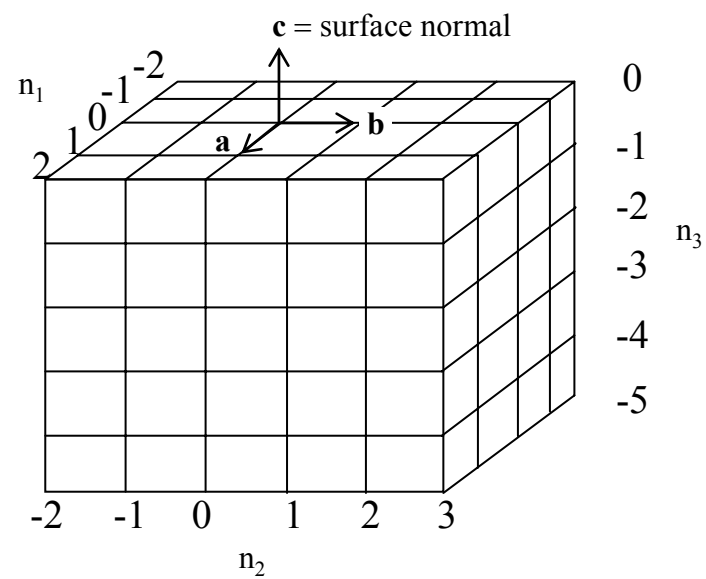

$$I \propto N_1^2 N_2^2 \left|F_c(HKL)\right|^2 \left|F_{CTR}(L)\right|^2$$

$$\left|\mathrm{Fctr}\right|^2 = \frac{1}{4\sin^2(\pi L)}$$

This is the origin of the crystal truncation rod:

- For integer H and K intensity is proportional to $N_1 x N_2 x F_{ctr}(L)$
- For non-integer H and K, S_1 and S_2 ~0, i.e. no sharp boundary in-plane
- Therefore, rods only occur in the direction perpendicular to the surface (n_3 direction)

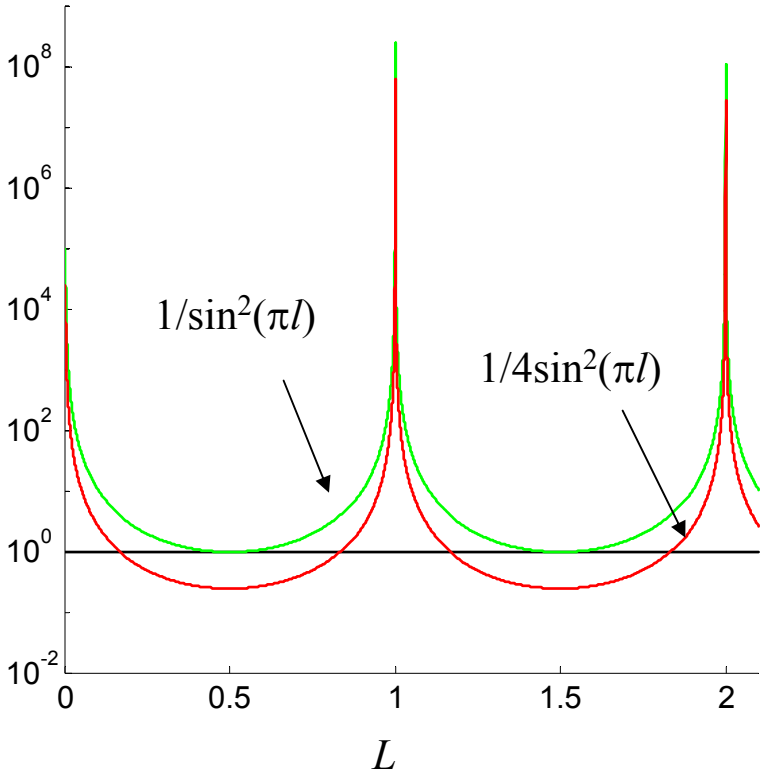

F_{ctr} lower at anti-Bragg than finite xtal. Why? Finite xtal has scattering from two sides, CTR is only from one side.

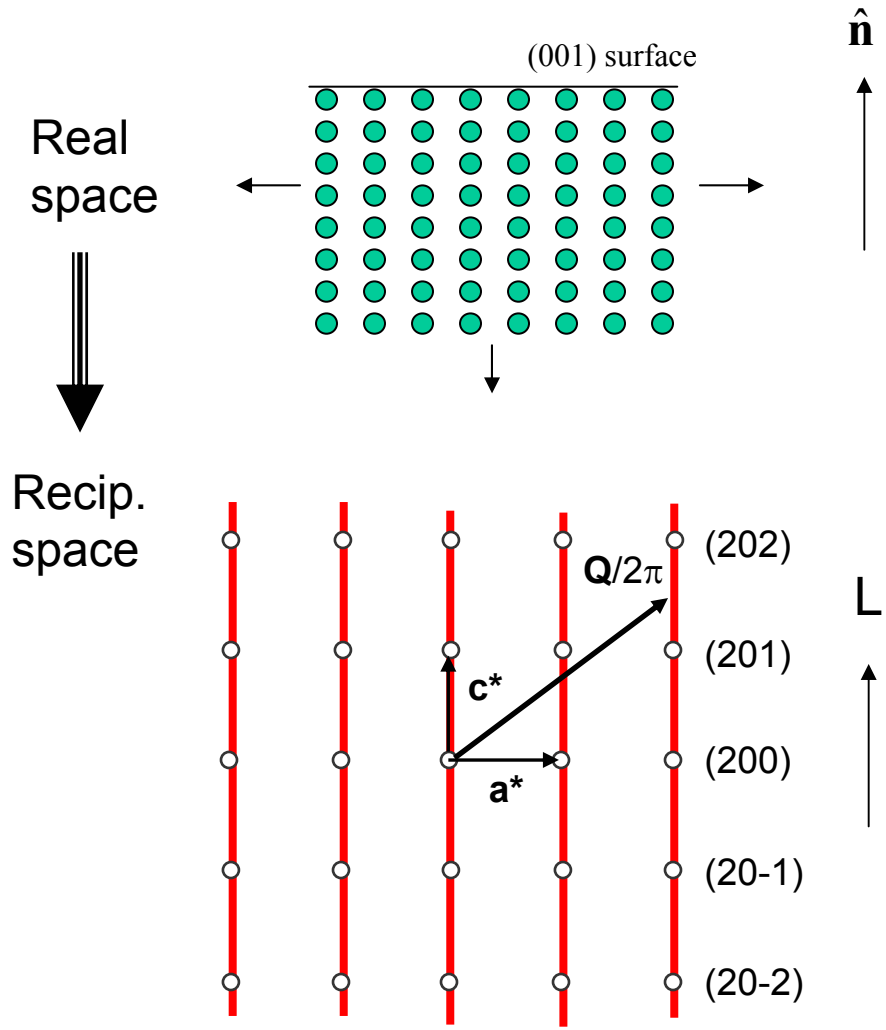

The scattering between Bragg peaks along a CTR results from a sharp termination of the crystal, and has a well defined functional form. But what does that tell us about the interface structure?

$$I \propto N_1^2 N_2^2 \left|F_c(HKL)\right|^2 \left|F_{CTR}(L)\right|^2$$

F_c contains all the structure information (e.g. atomic coordinates). But so far we've assumed all cells are structurally equivalent. What if we add a surface cell with a different structure factor?

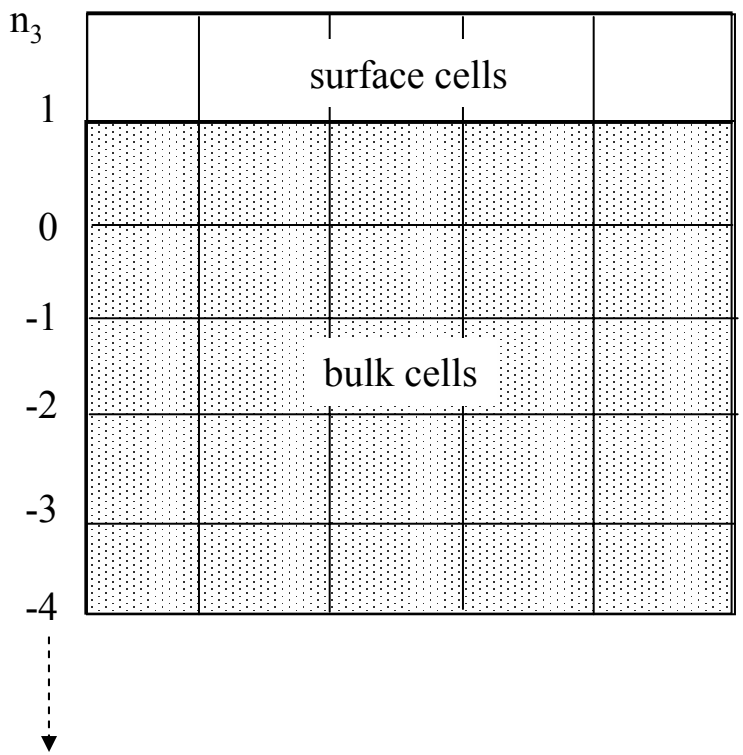

$$E_T = E_{bulk} + E_{surf}$$

$$E_{bulk} = N_1 N_2 \, F_{c,\,bulk}(HKL) \, F_{CTR}(L)$$

$$E_{surf} = N_1 N_2 \, F_{c,\,surf}(HKL) \, e^{i2\pi L}$$

Therefore final expression:

$$I \propto N_1^2 N_2^2 \left| F_{bulk,c} F_{CTR}(L) + F_{surf,c} \right|^2$$

$$F_c = \sum_{j=1}^{n} f_j e^{i\,\mathbf{Q}\bullet\mathbf{r}_j} e^{-M_j} \qquad \mathbf{Q}\bullet\mathbf{r}_j(xyz) = 2\pi(x\,H + y\,K + z\,L)$$

- In the mid-zone between Bragg peaks F_{CTR} ~1
- Therefore the "bulk" scattering and "surface" are of similar magnitude between Bragg peaks, ie sensitive to **one** bulk cell (modified by F_{ctr}) and **one** surface cell
- The "surface" and "bulk" sum in-phase (i.e. interfere if F_{surf}, different from F_{bulk})
- Near Bragg peak the surface is completely swamped:

  $I_{Bragg} / I_{CTR} > 10^5$

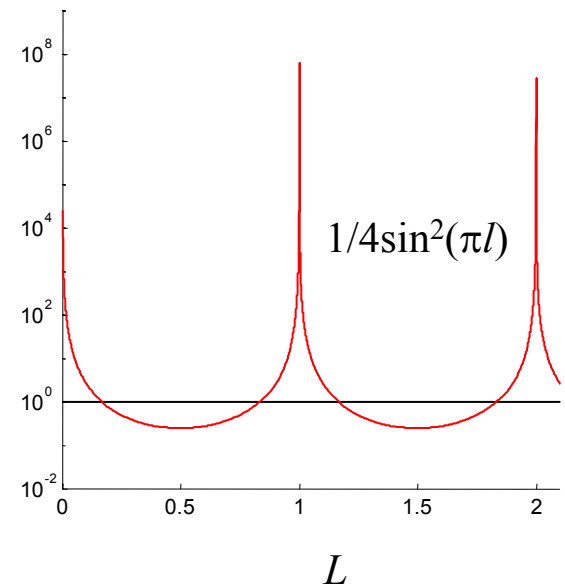

Influence of surface structure:

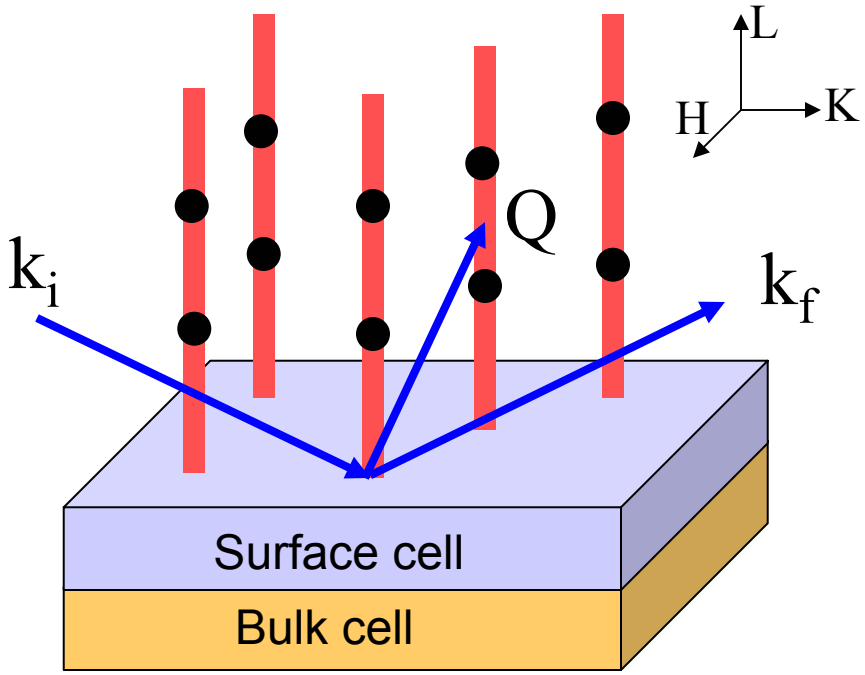

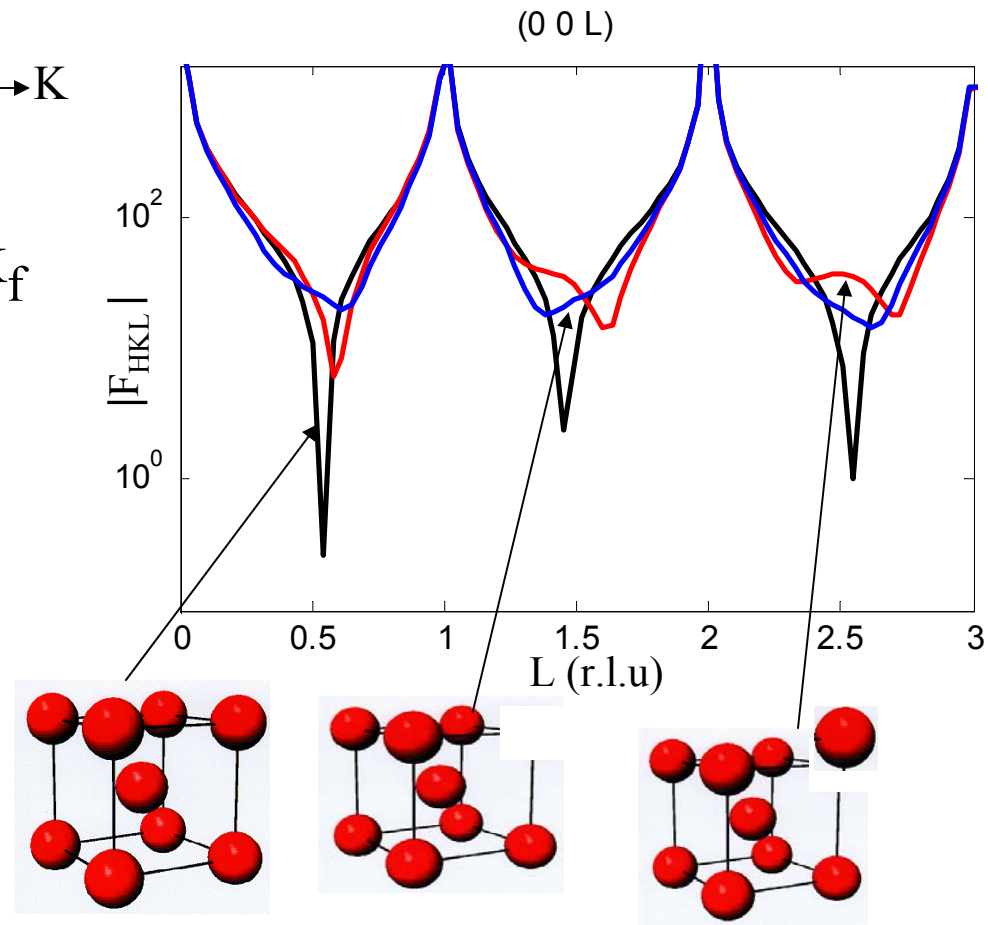

Known bulk structure and modifiable surface cell

$$I \propto N_1^2 N_2^2 \left| F_{bulk} F_{CTR}(L) + F_{surf} \right|^2$$

Simulation of CTR profiles for a BCC bulk and surface cell for (001) surface showing sensitivity to occupancy and displacements

Influence of surface structure:

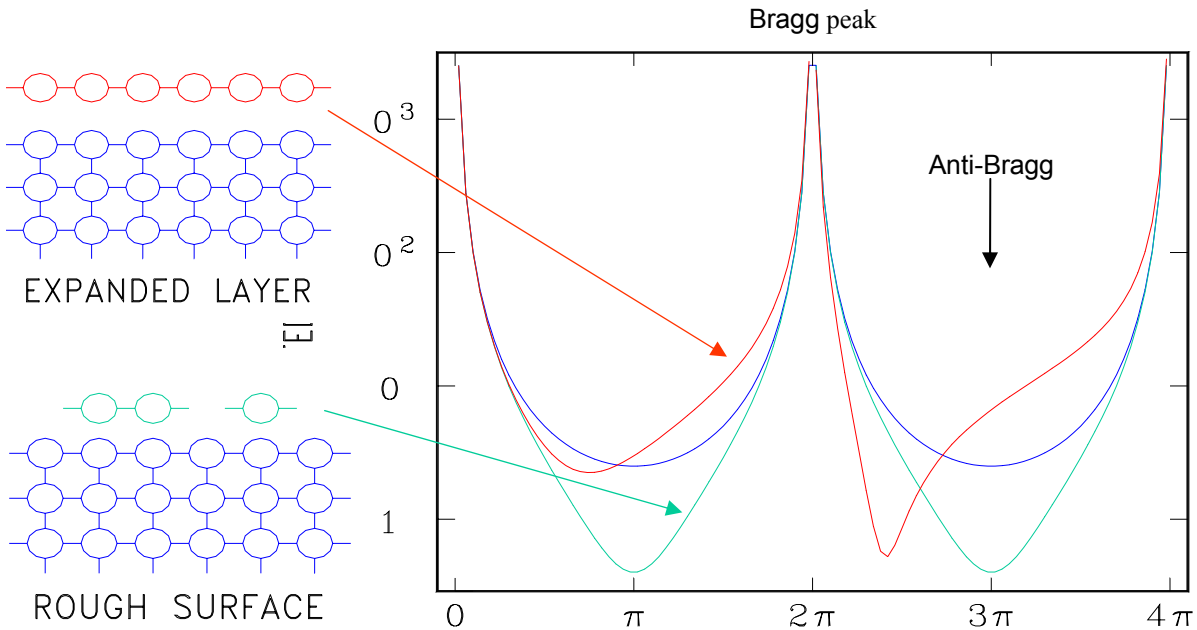

Observe several orders of magnitude intensity variation with changes in surface:

- atomic site occupancy
- relaxation (position)
- presence of adatoms
- roughness

Roughness “kills” rod intensity

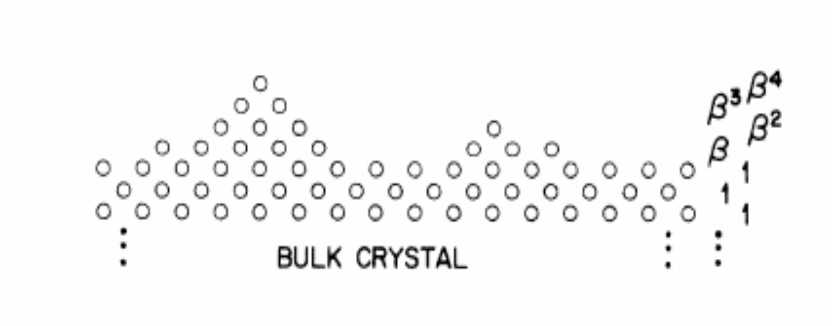

Interference between different height features cause destructive interference

Robinson β model

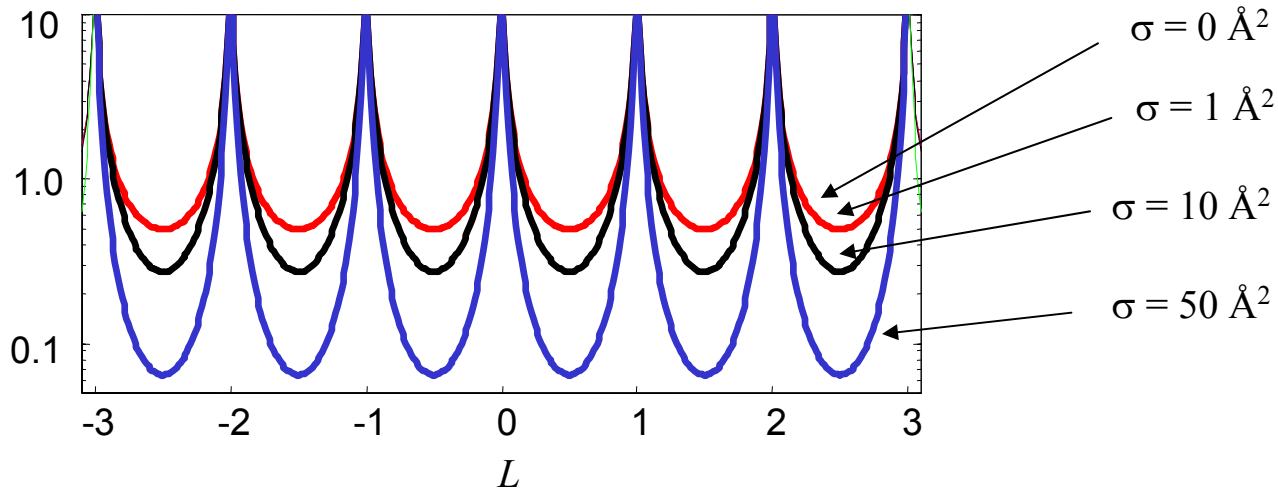

Distinguish roughness from structure because roughness is uniform decrease in intensity

Simulations of Pb/Fe_2O_3

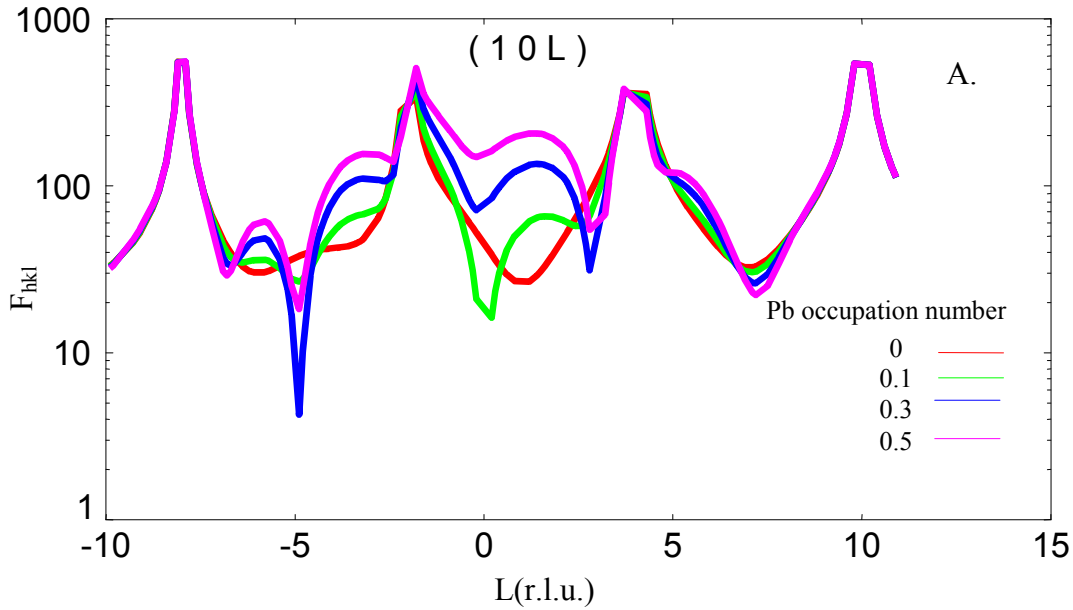

A. Calculations as a function of surface coverage

B Calculations as a function of the z-displacement (along the c-axis), the Pb occupation number is fixed at 0.3.

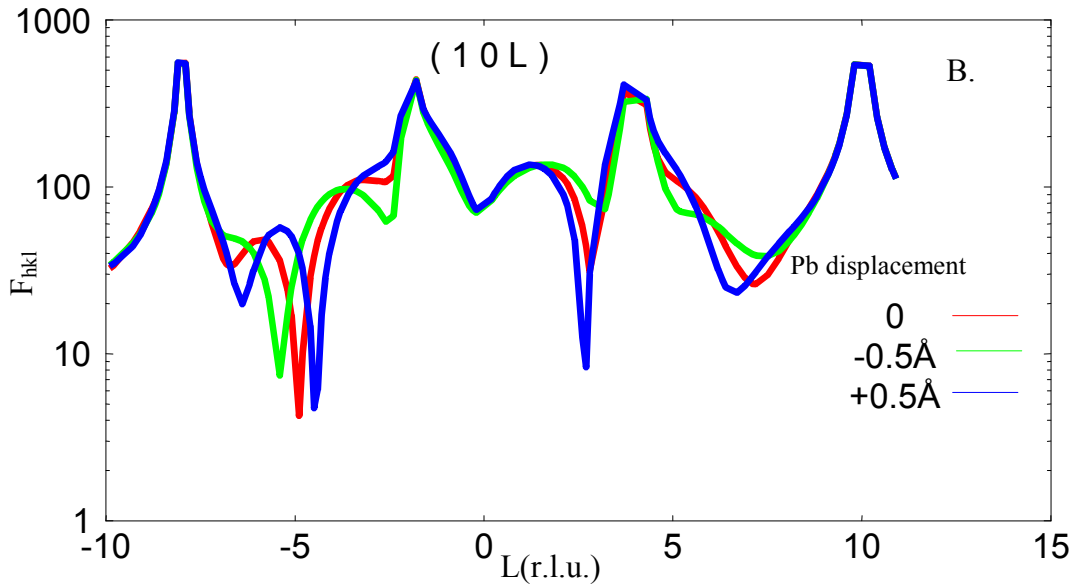

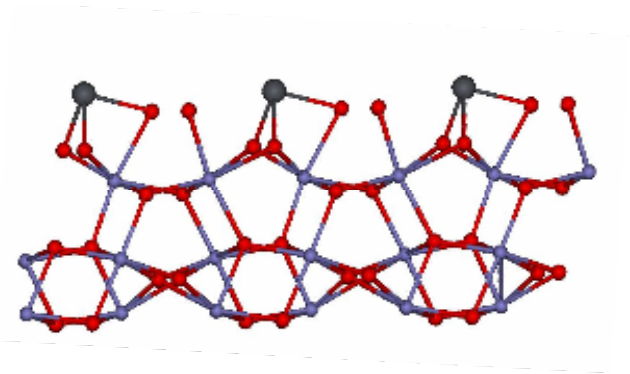

Surface scattering measurement:

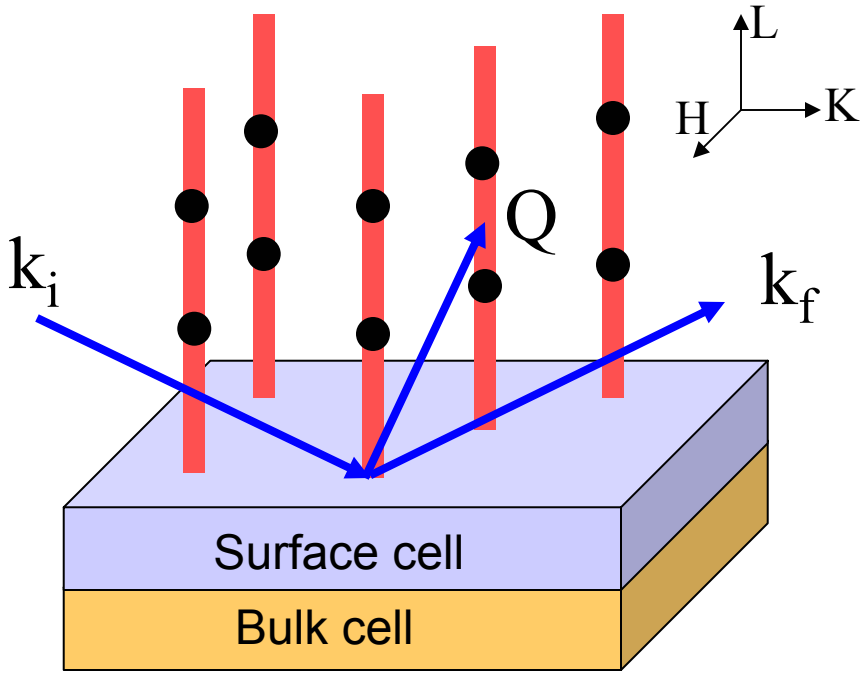

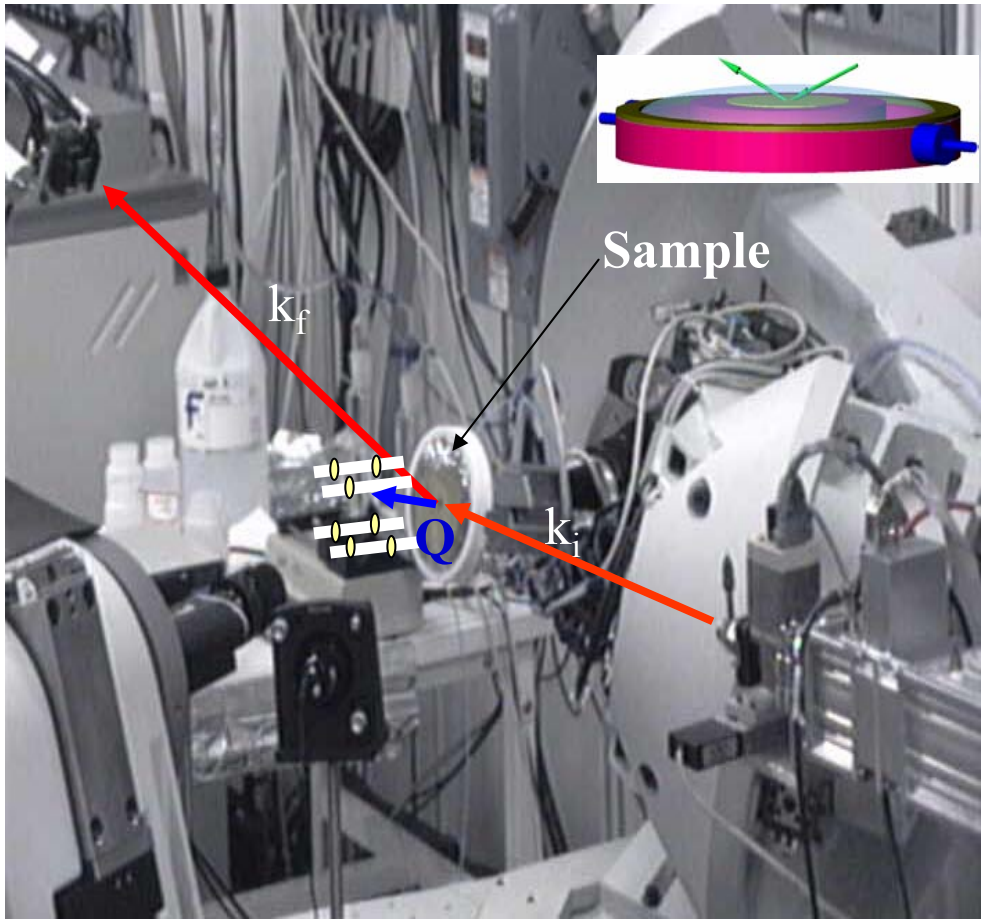

Six circle Kappa geometry diffractometer (Sector 13 APS)

Goal is to measure the intensity profile along one or more rods.

Sample orientation controls reciprocal lattice orientation.

Detector controls **Q**

An incomplete list of practical details

1. What do you need:
   - High quality (mono-lithic) crystal (mosaic kills intensity)
     - Sample sizes from 1mm to several cm
   - High quality surface (roughness kills intensity)
   - Goniometer and synchrotron
   - Know your bulk lattice parameters, coordinate system for surface and Q's of allowed Bragg peaks
   - Simulate before you measure
2. Sample orientation:
   - Find the optical surface (similar to reflectivity)
   - Find bulk reflections (usually you know the approximate direction of the surface normal so "dummy in" a reflection. Then hunt….
3. Check your rod intensity and alignment
   - Miss-cut results in tilted rods: plan your scans accordingly
   - Check for reconstruction/surface symmetry

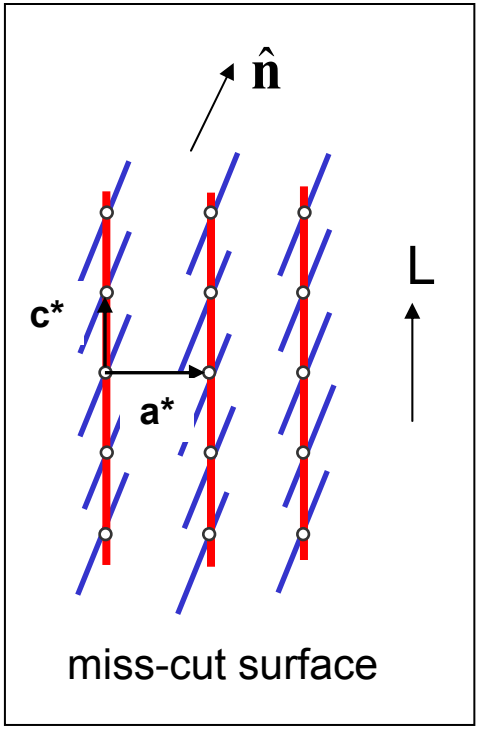

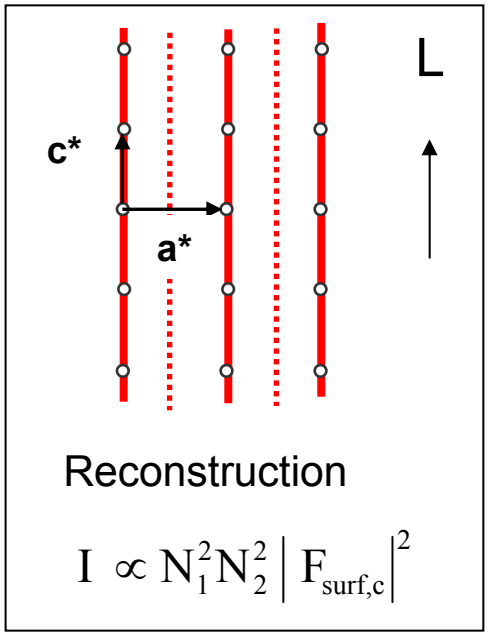

What's the best way to figure out what rods to measure, what reflections to look for to align? Make a map!

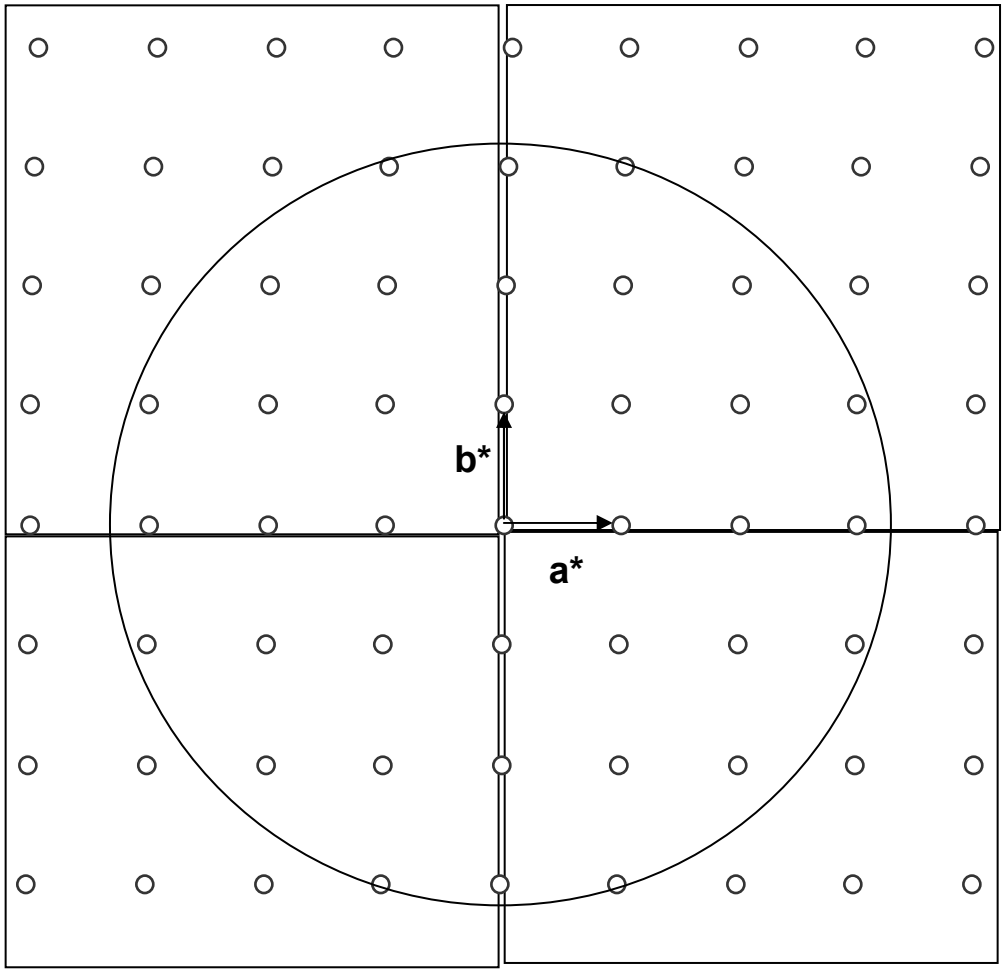

- What's the symmetry of reciprocal space?
- Where are the Bragg peaks on the rod?
- Whats Q max?

- How far to scan in L?
  - Min to max
- What rods to measure?
  - *(00L)* gives you z-information
  - *(HKL)* gives you x,y,z information

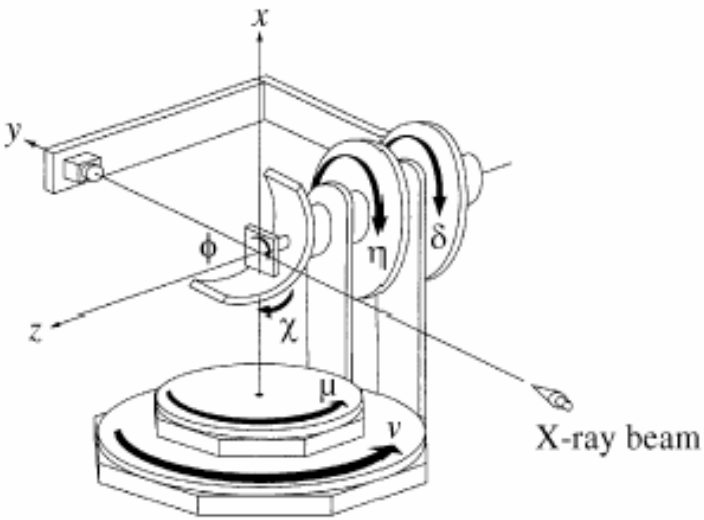

Multi-axis goniometer allows high degree of flexibility to access surface scattering features (from You, 1999)

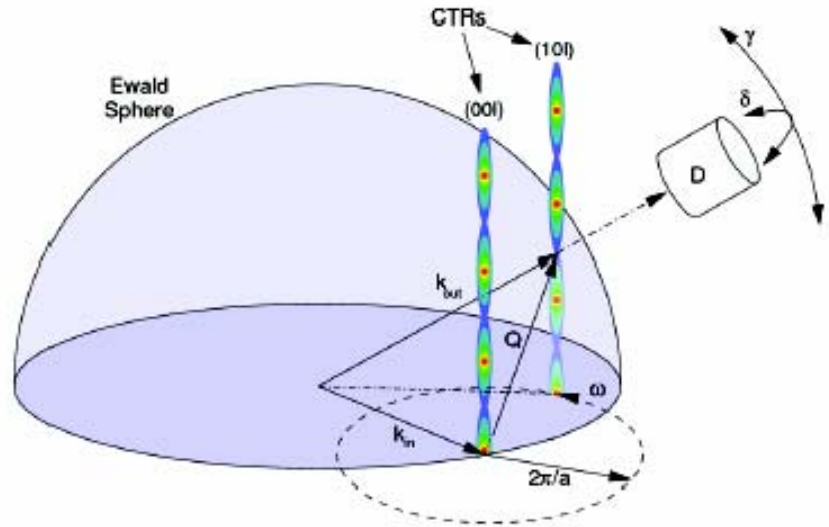

Scattered intensity is measured when the rod intersects the Ewald Sphere (from Schleputz, 2005)

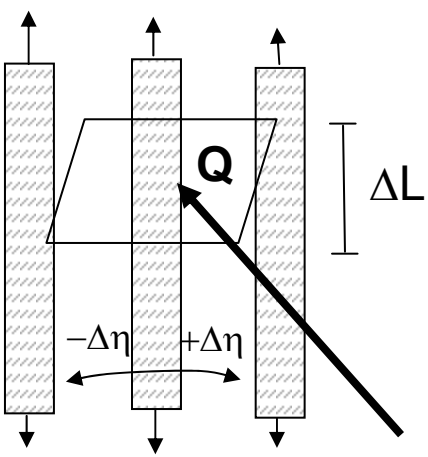

Generally not too worried about ΔL since rods are "slowly varying"

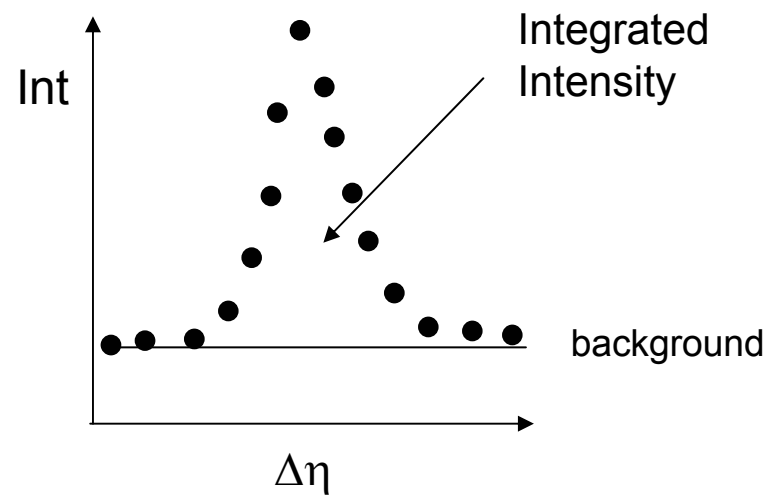

Scan of rod through resolution function

Measurement by rocking scans:

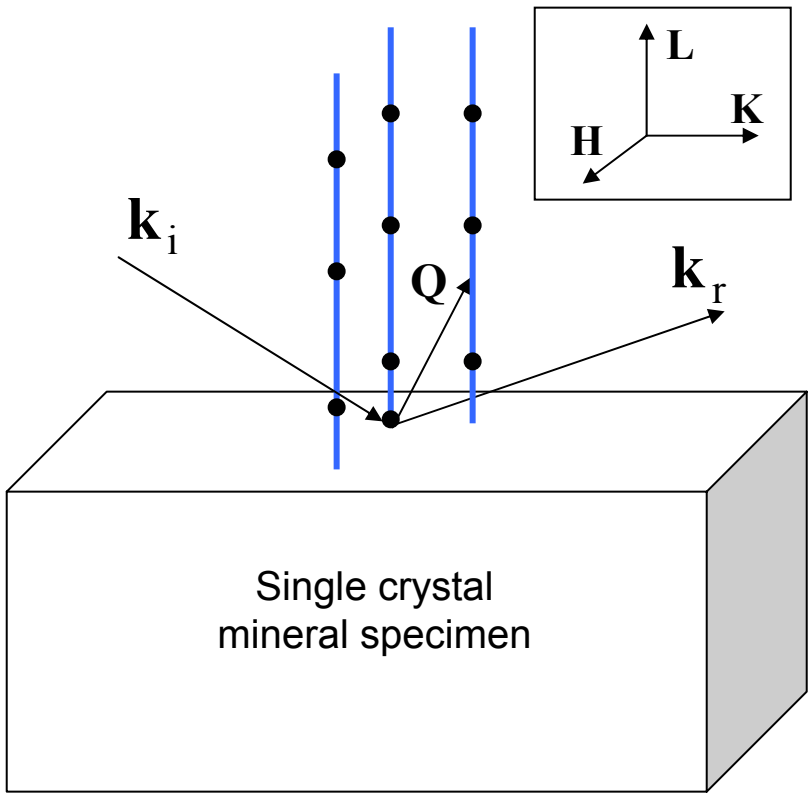

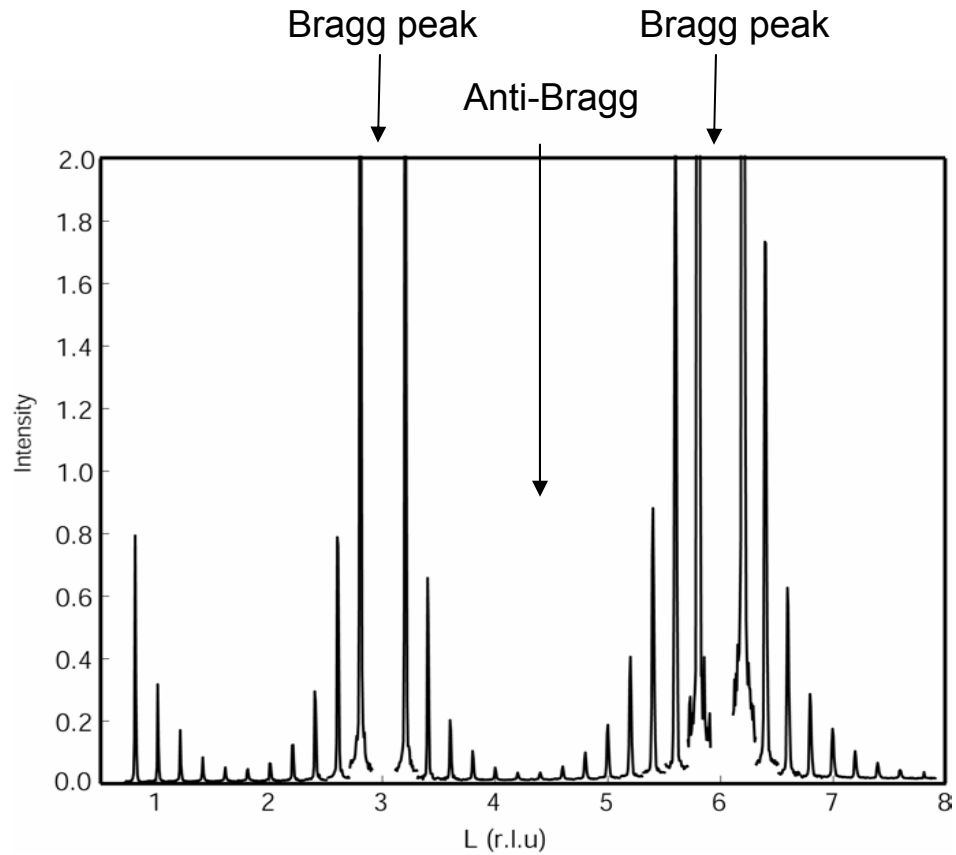

- Given a fixed **Q** rock the sample so the rod cuts through Ewald sphere: provide an accurate measure of the integrated intensity
- Integrated intensity is corrected for geometrical factors to produce experimental structure factor (F_E) for comparison with theory → e.g. lsq model fitting
- Symmetry equivalents are averaged to reduce the systematic errors

Sample cells/environmental chambers:

- Stable surface can be run in air
- UHV chamber/film growth scattering chamber
- Liquid / controlled atmosphere scattering cell

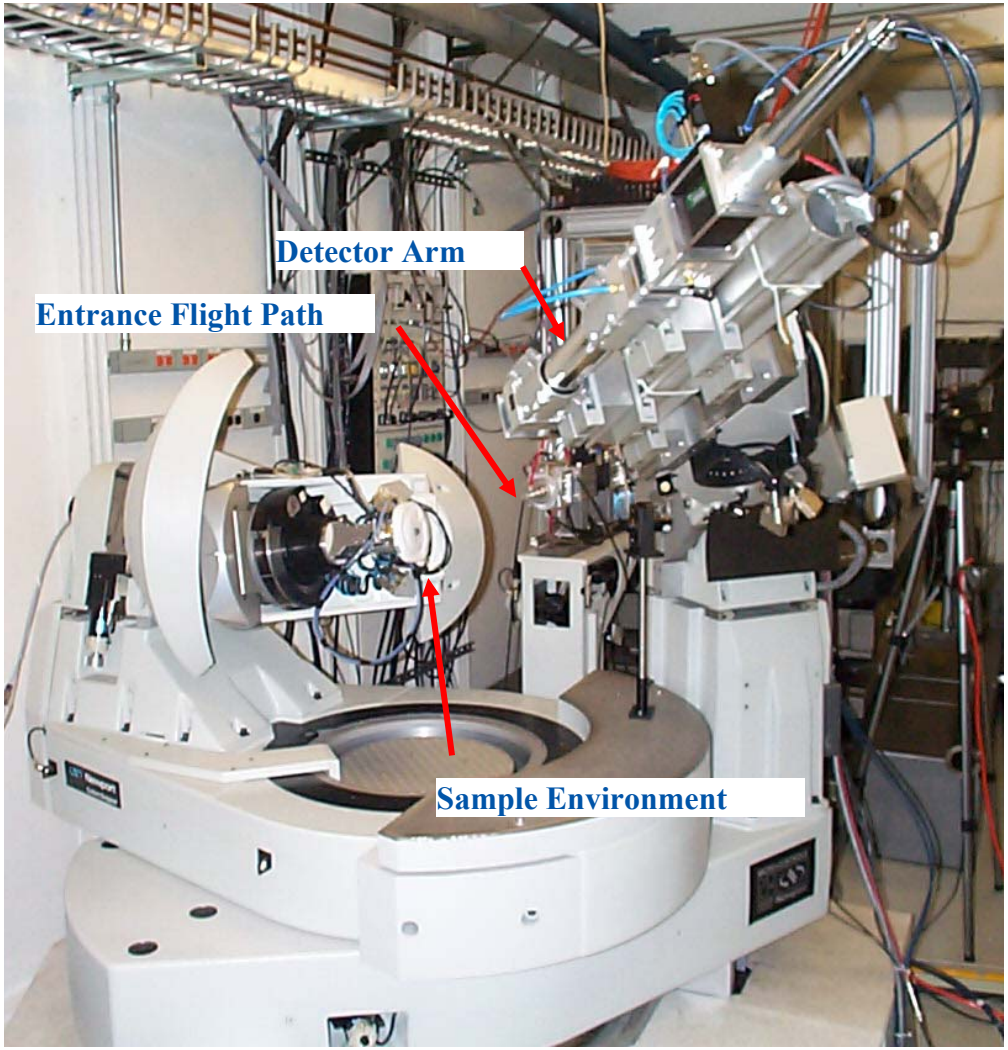

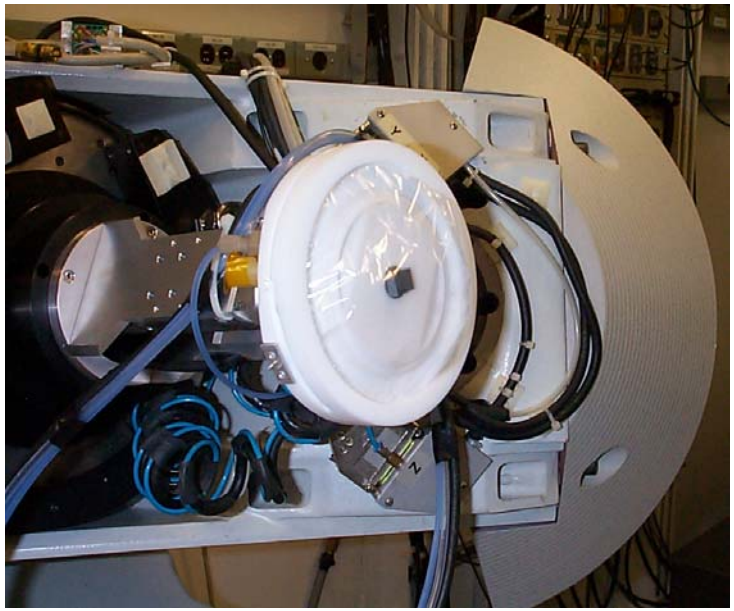

General Purpose Diffractometer (APS sector 13)

- Large Kappa-geometry six circle diffractometer
  - Leveling table with 5-degrees of freedom
  - High angular velocity (up to 8 deg/sec)
  - Small sphere of confusion (< 50 microns)
  - On the fly scanning

- Open sample cradle, capable of supporting large sample environments weighting up to 10kg.
  - Liquid/solid environment cells.
  - Diamond Anvil Cell (DAC)
  - Small UHV Chamber
  - High temperature furnace

- Open geometry also allows for mounting solid state fluorescence detectors and beam/sample viewing optics on the Psi axis bench

- High load capacity detector arm supports a variety of detectors
  - Point detectors
  - CCD based area detectors
  - Analyzer crystal for high resolution diffraction and inelastic scattering

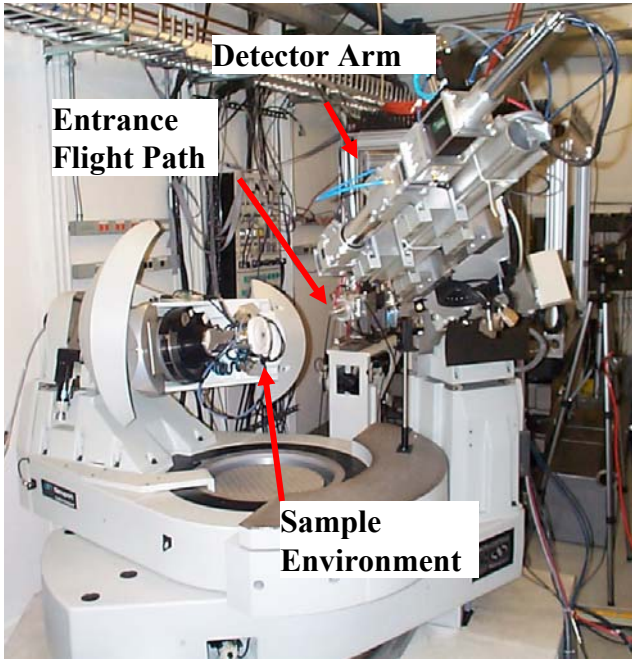

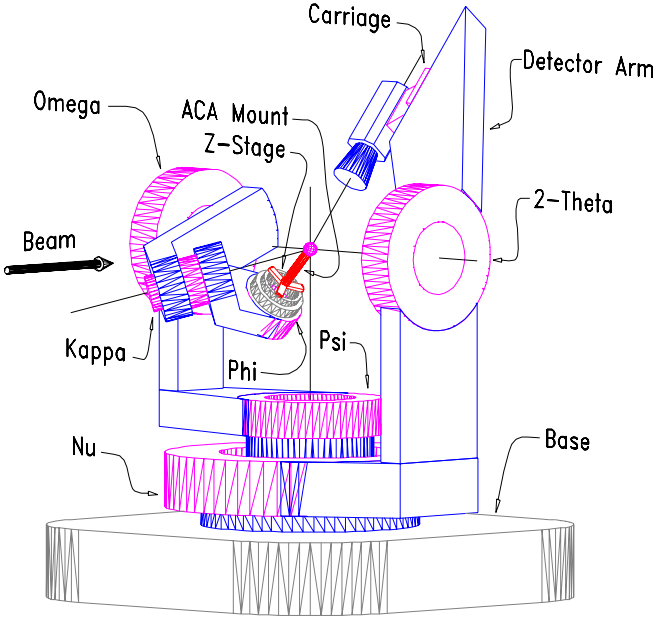

Liquid cells

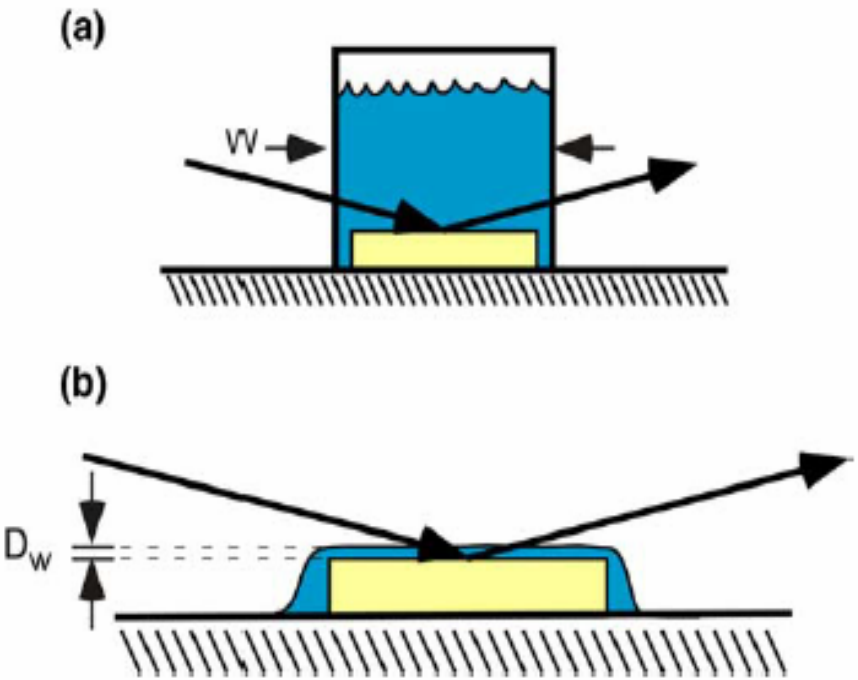

(a) Transmission and (b) thin film cells
(Fenter 2004)

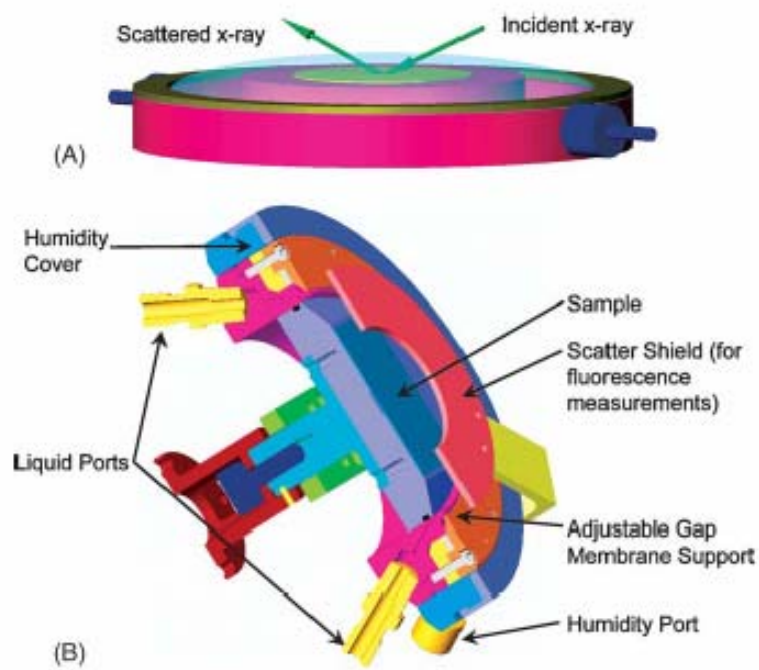

Fig. 5. Liquid cell sample geometry (A) showing X-rays interacting with the liquid interface region by penetrating a thin membrane and a liquid film. The liquid cell used in our measurements (B) is designed to allow the control of the inlet and outlet liquid flow and has a motorized adjustable film to surface gap to aid in creation of thin liquid layers. In addition to the liquid control a silver scattering mask shields the edges of the sample from the view of the florescence detector and humidified He "bag" prevents the sample from drying and reduces air scatter of the direct beam.

Example: Voltage dependant water structure at a Ag(111) electrode surface

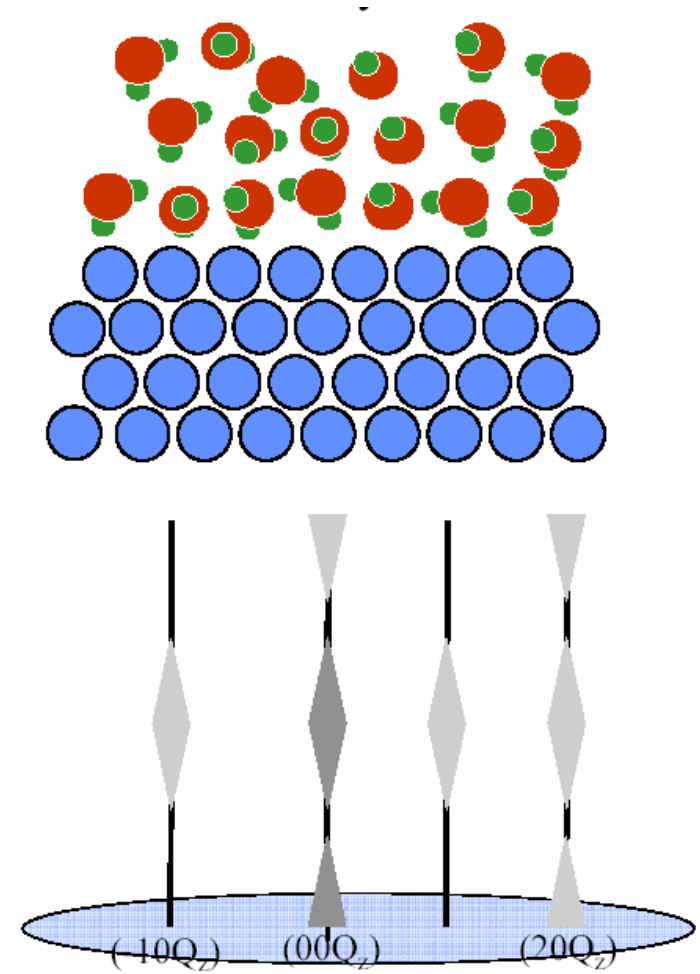

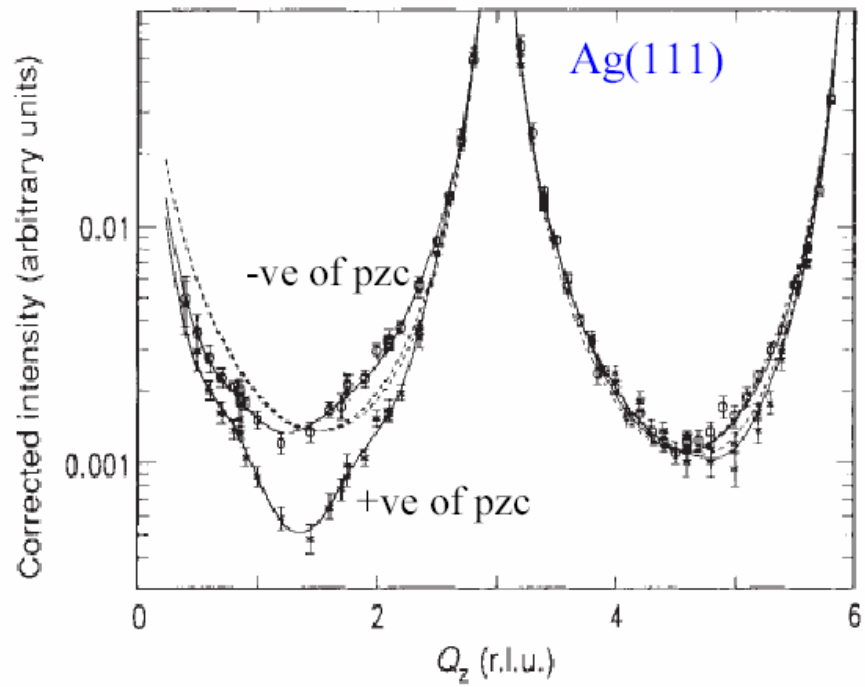

Toney et al., Nature **368**, 444 (1994)

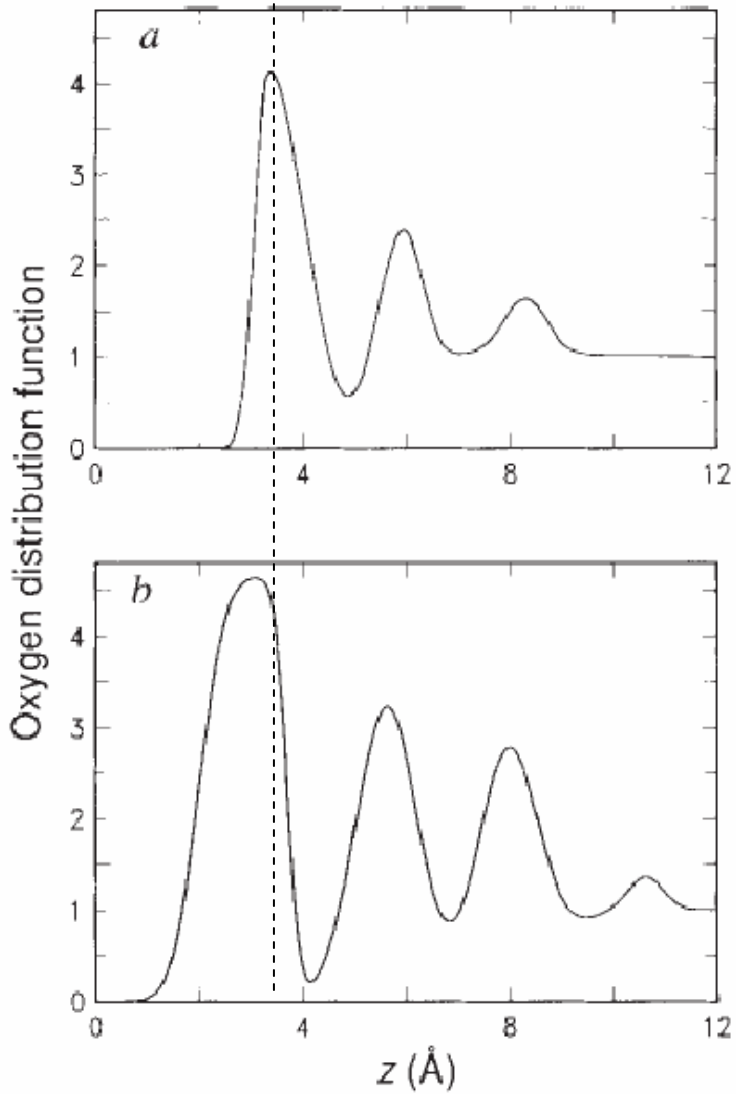
a
b
Oxygen distribution function
z (Å)
0
1
2
3
4
0
4
8
12

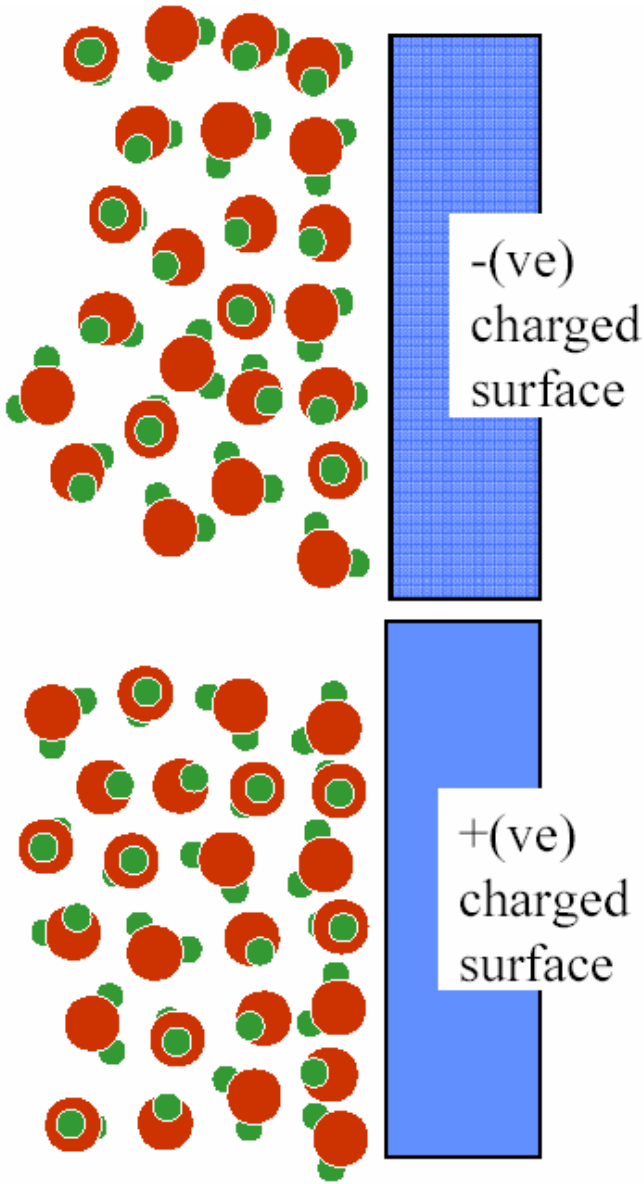
-(ve)
charged
surface
+(ve)
charged
surface

Example: Structure of Mineral-Water Interfaces

ELSEVIER

Available online at www.sciencedirect.com

SCIENCE DIRECT®

Progress in Surface Science 77 (2004) 171–258

Progress in SURFACE SCIENCE

www.elsevier.com/locate/progsurf

Review

Mineral–water interfacial structures revealed by synchrotron X-ray scattering ☆

Paul Fenter [a,*], Neil C. Sturchio [b]

[a] *Argonne National Laboratory, ER-203, 9700 South Cass Avenue, Argonne, IL 60439, USA*
[b] *Department of Earth and Environmental Sciences, University of Illinois at Chicago, 845 West Taylor Street, Chicago, IL 60607, USA*

Abstract

Chemical reactions occurring at the mineral–water interface are controlled by an interfacial layer, nanometers thick, whose properties may deviate from those of the respective bulk mineral and water phases. The molecular-scale structure of this interfacial layer, however, is poorly constrained, and correlations between macroscopic phenomena and molecular-scale processes remain speculative. The application of high-resolution X-ray scattering techniques has begun to provide substantial new insights into the molecular-scale structure of the mineral–water interface. In this review, we describe the characteristics of synchrotron-based X-ray scattering techniques that make them uniquely powerful probes of mineral–water interfacial structures and discuss the new insights that have been derived from their application. In particular, we focus on efforts to understand the structure and distribution of interfacial water as well as their dependence on substrate properties for major mineral classes including oxides, carbonates, sulfates, phosphates, silicates, halides and chromates. We compare these X-ray scattering results with those from other structural and spectroscopic techniques and integrate

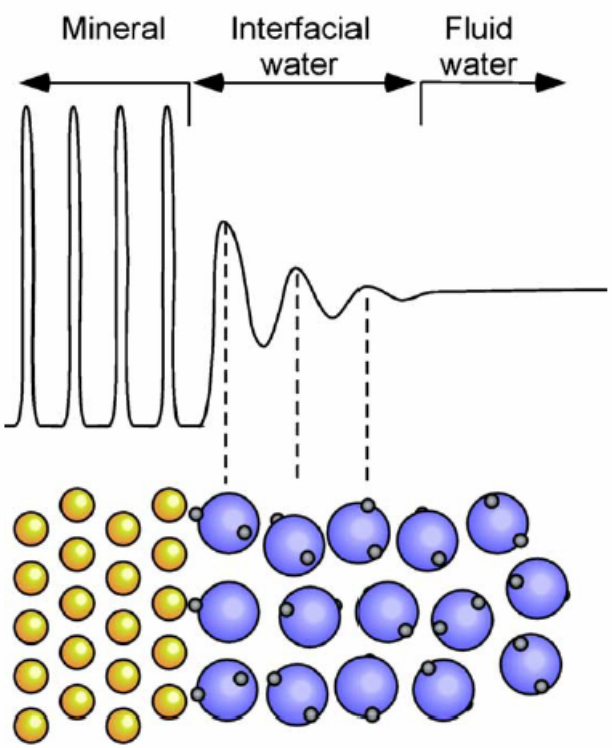

Example: Hydrated vs. UHV prepared α-Al_2O_3 (0001) surface

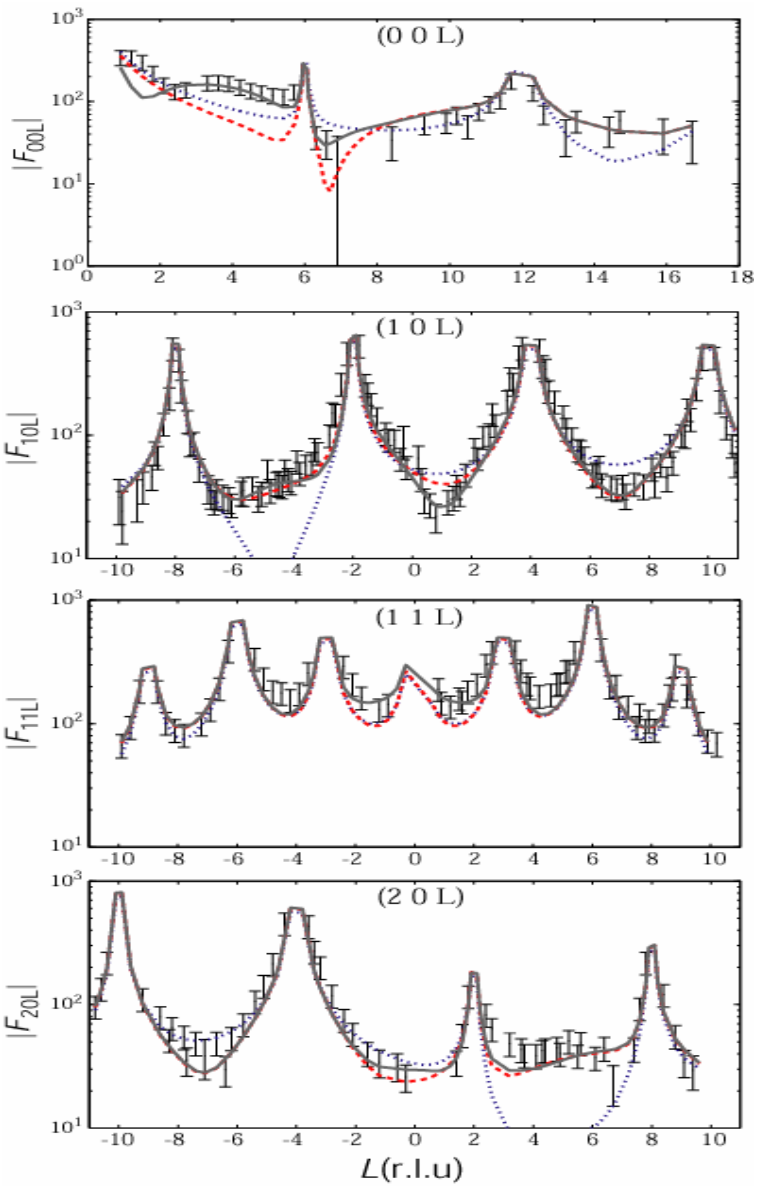

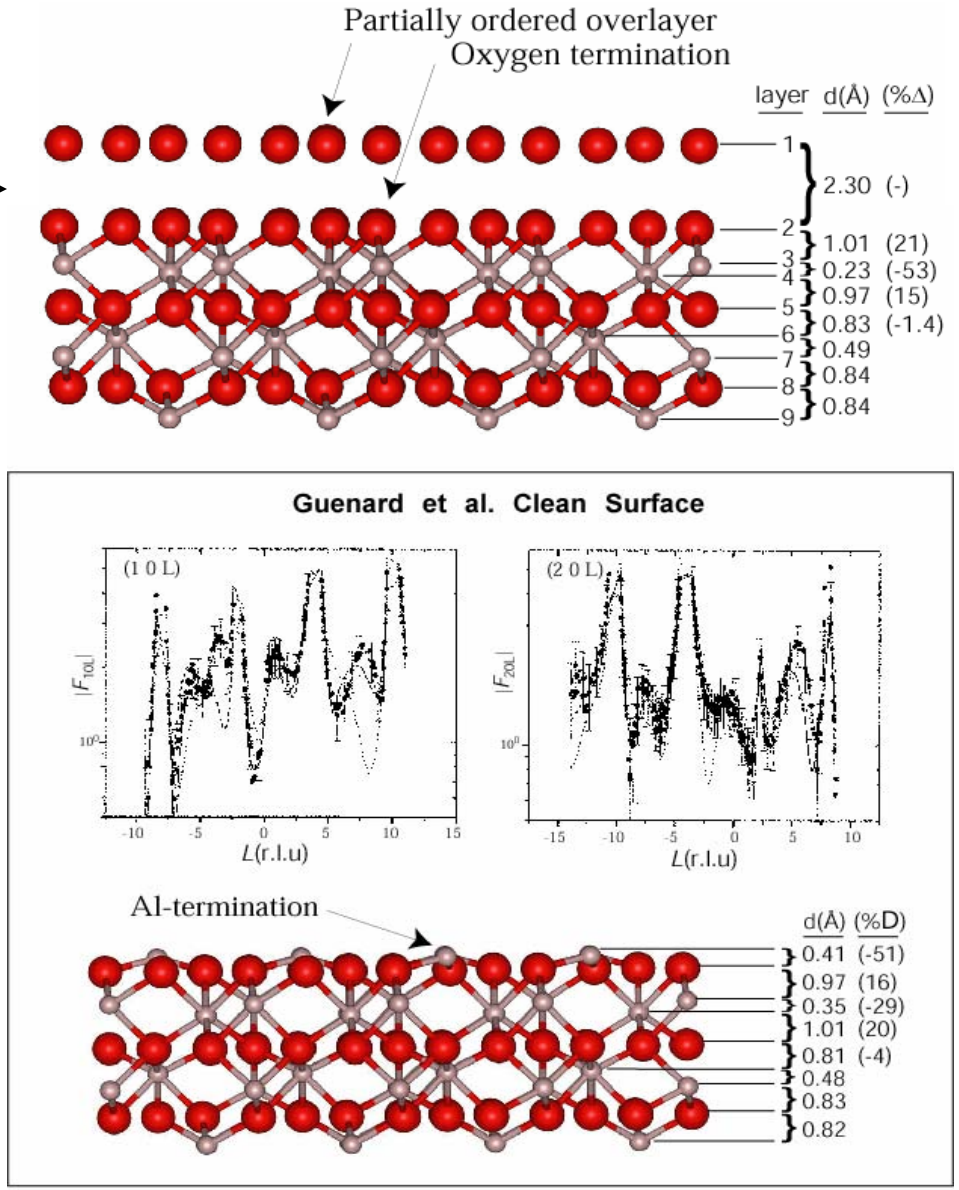

(Eng et al., (2000) *Science*, **288** 1029)

(Guenard et al., (1997) *Surf. Rev. Lett.*, **5** 321)

Example: Ordering in Thermally Oxidized Silicon

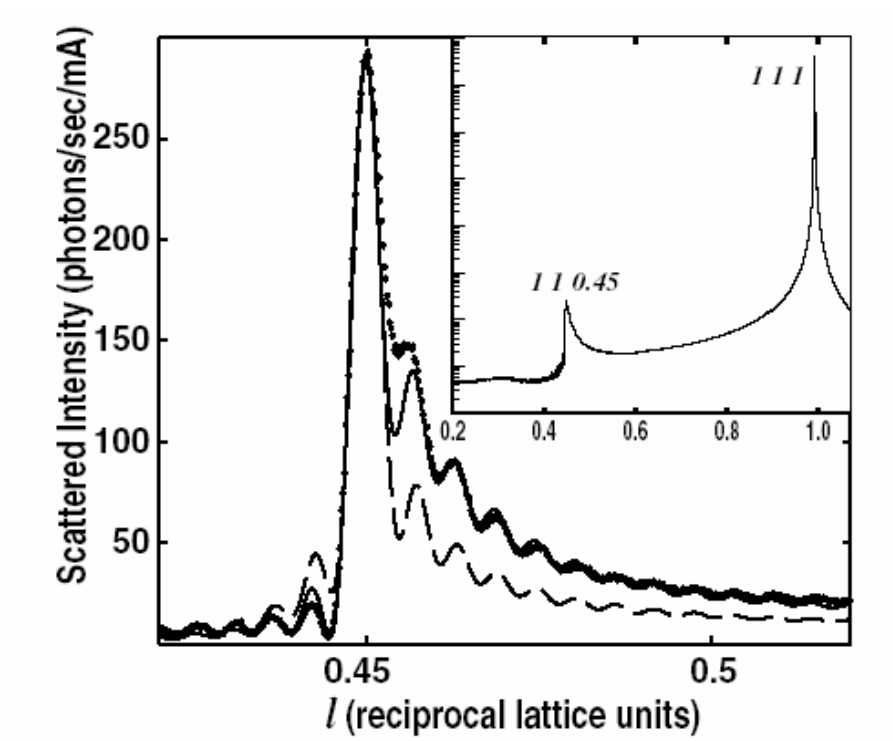

FIG. 1. Scattered intensity from a steam oxide on Si(001) is shown as dots. The solid line is the fit using an expansion of the silicon atoms which increases towards the surface, and the dashed line is the fit with a constant expansion throughout the oxide. The inset is the scattered intensity on a log scale along the entire 111 CTR, including the 111 Bragg peak.

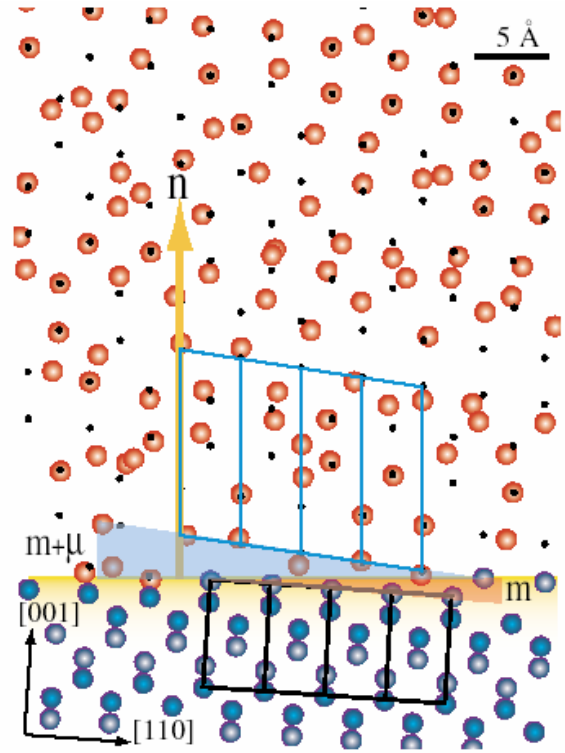

FIG. 3 (color). Illustration of the silicon positions near the Si-SiO_2 interface for a 4° miscut projected onto the $(\bar{1}10)$ plane. The silicon atoms in the substrate are blue and those in the oxide are red. The small black spots represent the translated silicon positions in the absence of static disorder. The silicon atoms in the oxide have been randomly assigned a magnitude and direction based on the static disorder value at that position in the lattice. The outline of four silicon unit cells is shown in black, whereas the outline of four expanded lattice cells in the oxide is shown in blue.

A. Munkholm and S. Brennan (2004) *Phys Rev. Lett.* **93** 036106

Some new stuff

Inversion algorithms for rapid determination of interfacial electron density profiles

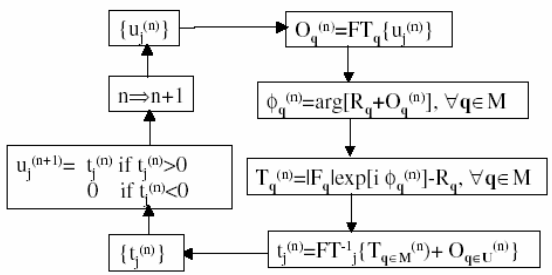

Figure 1. The flow chart of the RECURSION algorithm that converts an input real-space distribution $\{u_j^{(n)}\}$ to an output distribution $\{t_j^{(n)}\}$ by constraining the Fourier-transformed quantities to experimental amplitude data. The new input real-space distribution $\{u_j^{(n+1)}\}$ for the next iteration of the feedback loop is calculated from the output distribution at the previous iteration by *object-domain operations* that ensure that this is the closest possible to the output that satisfies the condition of non-negativity.

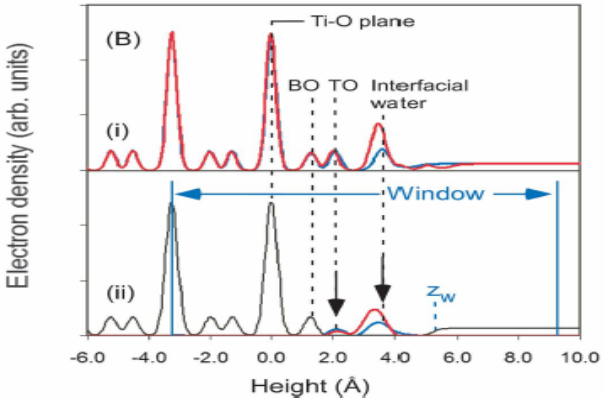

Anomalous (E-dependant) surface scattering: phase constraints/chemical information

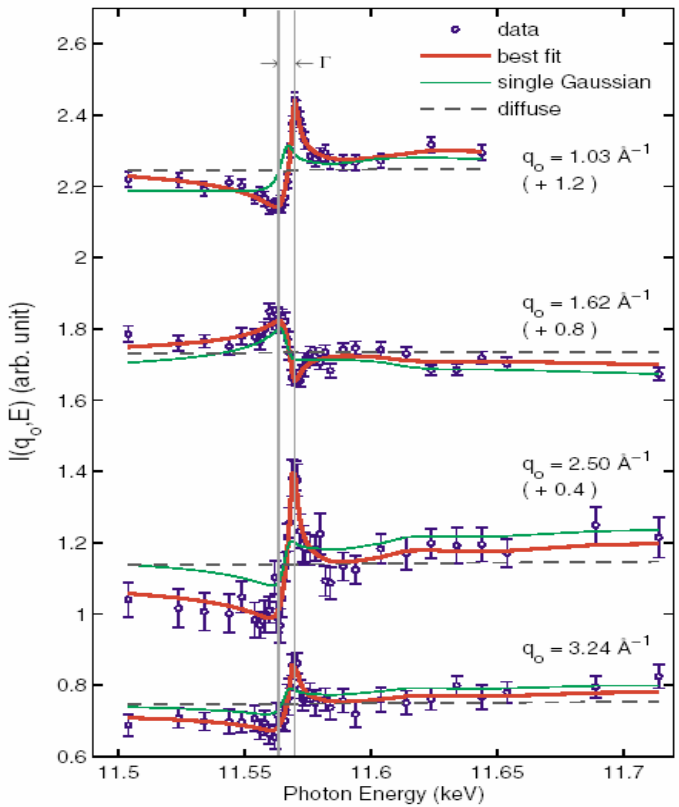

FIG. 2 (color). RAXR spectra normalized with nonresonant reflectivity near the Pt L_{III} edge (11.564 keV) of the quartz(100)-PTA interface at selected momentum transfers. Lines represent calculations corresponding to the best-fit model (red thick lines) and two other models described in the text. The vertical lines indicate the energies noted in Fig. 3(b). Data are offset vertically as indicated for clarification.

Fenter and Zhang (2005) *Phys. Rev. B*, 081401.
Saldin et. al. (2001-2002) *J Phys Cond Matt*
Baltes et. al. (1997) Phys. Rev. Lett
Tweet D. J., et. al. (1992) *Physical Review Letters* **69**(15), 2236-9.
Walker F. J. and Specht E. D. (1994) In. *Reson. Anomalous X-Ray Scattering*, 365-87.
Park et. al. (2005) *Phys Rev. Lett.*, 076104

Pixel array detectors with high dynamic range and fast readout means data collection speedup 10x or more

Acta Crystallographica Section A
Foundations of Crystallography
ISSN 0108-7673

Received 31 January 2005
Accepted 9 May 2005

Improved data acquisition in grazing-incidence X-ray scattering experiments using a pixel detector

C. M. Schlepütz, R. Herger, P. R. Willmott,* B. D. Patterson, O. Bunk, Ch. Brönnimann, B. Henrich, G. Hülsen and E. F. Eikenberry

Swiss Light Source, Paul Scherrer Institute, CH-5232 Villigen, Switzerland. Correspondence e-mail: philip.willmott@psi.ch

The use of an area detector in grazing-incidence X-ray experiments lends many advantages in terms of both speed and reliability. Here a discussion is given of the procedures established using the PILATUS pixel detector developed at the Swiss Light Source for optimizing data acquisition and analysis of surface diffraction data at the Materials Science beamline, especially with regard to reflectivity measurements, crystal truncation and fractional order rods, and grazing-incidence diffraction experiments.

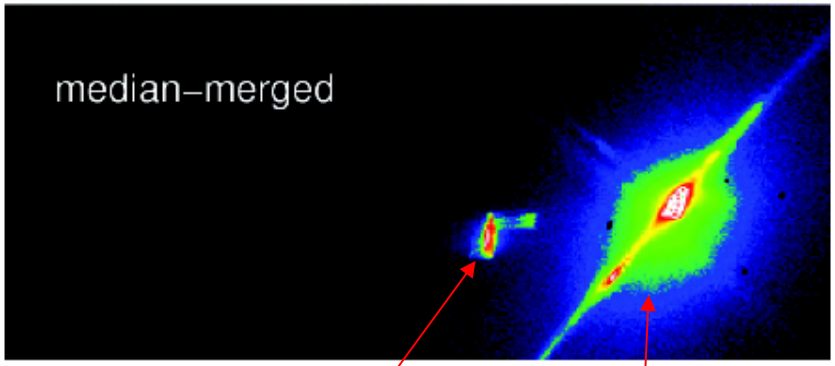

CTR intersecting Ewald Sphere

TDS from nearby Bragg peak

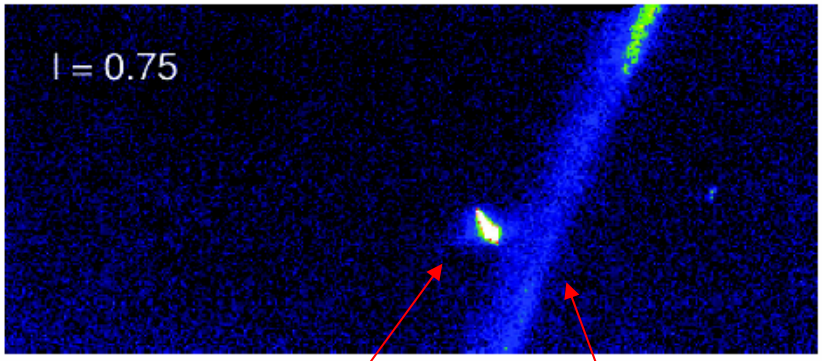

CTR intersecting Ewald Sphere

Powder ring

References (a very incomplete list)

Reference texts:

Warren B.E. (1969) *X-ray Diffraction*. New York: Addison-Wesley.
Als-Nielsen J. and McMorrow D. (2001) *Elements of Modern X-ray Physics*. New York: John Wiley.
Sands D.E. (1982) *Vectors and Tensors in Crystallography*. New York: Addison-Wesley.

A few surface scattering methods papers:

Robinson I. K. (1986) *Phys. Rev. B* **33**(6), 3830-3836. (→ original reference)
Andrews S.R. and Cowley R.A. (1985) *J. Phys C.* **18**, 642-6439. (→ original reference)
Vlieg E., et. al. (1989) *Surf. Sci.* **210**(3), 301-321.
Vlieg E. (2000) *J. Appl. Crystallogr.* **33**(2), 401-405. (→ rod analysis code)
Trainor T. P., et. al.. (2002) *J App Cryst* **35**(6), 696-701. (→ rod analysis code)
Fenter P. and Park C. (2004) *J. App Cryst* **37**(6), 977-987.
Fenter P. A. (2002) *Reviews in Mineralogy & Geochemistry* **49**, 149-220.

Reviews

Fenter P. and Sturchio N. C. (2005) *Prog. Surface Science* **77**(5-8), 171-258.
Renaud G. (1998) *Surf. Sci. Rep.* **32**, 1-90.
Robinson I.K. and Tweet D.J. (1992) *Rep Prog Phys* **55**, 599-651.
Fuoss P.H. and Brennan S. (1990) *Ann Rev Mater Sci* 20 365-390.
Feidenhans'l R. (1989) *Surf. Sci. Rep.* **10**, 105-188.

Coordinate transformations, reciprocal space, diffractometry

You H. (1999) *J. App Cryst.* **32** 614-623.
Vlieg E. (1997) *J. Appl. Crystallogr.* **30**(5), 532-543.
Toney M. (1993) *Acta Cryst* **A49**, 624-642.
…. And many more….